Triangle Documentation
Part III – Trajectory Model Output
Using
Shannon Information Theory
by

J.A. Galt
D. L. Payton
Renn Hanson

February, 2017

Paper can be found online at:
http://www.genwest.com/Publications/genwestpublications/

Abstract

Lagrangian trajectory models or mixed Lagrangian – Eulerian trajectory models are commonly used in environmental studies. This is particularly true in applications studying accidental spills during emergency responses or planning for them. Model output is typically presented as mappings of the predicted time dependent locations of Lagrangian particles (Lagrangian Elements – LEs). Although these maps are familiar to most responders and are qualitatively useful they fall far short of presenting the quantitative information that can be obtained by an Eulerian analysis of the original model output. A description of this process was presented in the first two parts of this study (Galt, 2011; Galt, 2015).

This study, the third in the series, goes an additional step and examines the Lagrangian model output as represented by a classical Shannon communication channel (Shannon and Weaver, 1963). It is shown that the communication channel's information entropy can be linked to dominant physical processes within the Lagrangian model's geophysical domain. Each of the analytical processes leading from: 1) Lagrangian models particle distribution => 2) Eulerian densities => 3) Continuum density field => 4) Regional representation of probability densities => 5) Shannon information channel entropy are described with examples. A quantitative understanding of when the model loses information quality (i.e., needs more data) is the primary goal of this study.

Table of Contents

Introduction

Many models used to forecast the fate of pollutants use Lagrangian Elements (LEs) to represent the pollutant. The output from these represents “information”. The distribution of Lagrangian Elements evolve over time and provide the user with data about expected locations and concentrations of the dependent modeled variable. What is not so obvious is how to quantitatively understand how much information a model provides, how much the information degrades over time compared to some objective “base level”, and how, or when, data assimilation could be used to restore the “information content” of the model. For researchers and responders involved in trajectory analysis these are all important questions.

The objective of this study is to develop a quantitative definition of information content for a typical model framework using an information theory approach. This is done by considering the model output as a communication channel and investigating the amount of information that it can carry. The methods for calculating the capacity of the model's communication channel will be introduced and its evolution over time will be used to consider the answers to the questions posed in the preceding paragraph.

This analysis is carried out in a number of steps: 1) Initially, the Lagrangian point data is converted into an Eulerian density field. 2) The next step is to convert the Eulerian density field into a set of probability values. 3) The resulting probability densities will be used in Shannon's communication theorem (Shannon, 1963) to define the models information channel's entropy. 4) At this point it is shown that the maximum channel entropy is determined by the cardinality of the Eulerian density set and this places restrictions on the forms of Lagrangian to Eulerian conversion that is appropriate for step 1.

The final section of this study will be to investigate how the various geophysical processes typically simulated in a Lagrangian trajectory model are transformed into the evolution of the communication channel representing the model. These will be

discussed initially for idealized cases and then for realistic geophysical domains.

It is shown that the communication channel information entropy can be linked to dominant physical processes within the Lagrangian model's geophysical domain. Each of the analytical processes leading from: 1) Lagrangian models particle distribution => 2) Eulerian densities => 3) Continuum density field => 4) Regional representation of probability densities => 5) Shannon information channel entropy are described with examples.

Information Uncertainty and Entropy

In 1949 Claude Shannon, working on a mathematic theory of communication at Bell Laboratories, presented a classical paper which has appeared in a number of forms and was eventually published in a book. (Shannon and Weaver, 1963). In his research Shannon would describe a mathematical framework to quantify the information rate that a communication channel could carry. Or using a more modern term, bandwidth. He clearly defined the relationships between signal complexity, the probability of uncertainty, and redundancy. These were linked together in his definition of information entropy. At that time the focus of the study was telephone and telegraph lines and the effects of line noise on the information transmission rates. Shannon's work had immediate implication in the communication industry and fledgling computer studies.

In the decades since its introduction a whole field of “information theory” has been build up around Shannon's signal “uncertainty” and “entropy” and has found extensive applications in many fields such as artificial intelligence, data compression, and cryptanalysis, just to name a few. More general introductions to information theory can be found in many text books (Pierce,1980 and Roman,1997).

The remainder of this study will be based on Shannon's fundamental theorem relating channel entropy to signal probabilities.

$$Entropy = H(t) = -\sum_{j} p_j ln_2 p_j \qquad (1)$$

Shannon's concept of information entropy is strongly analogous to entropy used in physical chemistry as described in the laws of thermodynamics. In addition, it is closely linked to the concept of uncertainty in specifying the exact position of a Lagrangian particle. Shannon was quick to realize that the units of information entropy are binary numbers (bits) and like chemical entropy, information entropy is always measured relative to some value obtained at a maximum entropy state. In chemistry we speak of entropy relative to what it would be at absolute zero (0 deg. K). For information entropy an examination of equation (1) shows that the theoretical maximum value will occur when p_j is uniform over all of the (J) VOLUME elements. For this case, the maximum base information entropy will be $ln_2(J)$. All other possible entropies will be less than this maximum value and, in fact, this maximum value may not be obtainable in actuality if the cardinality of the VOLUME set is greater than the cardinality of the MASS set (J>N).

From this point on we will assume that the time dependent output from a Lagrangian trajectory model is viewed as an information channel and the model output has been converted into corresponding time dependent Eulerian density fields as outlined in the following section of this study. Applying these densities to formulate probabilities and using equation (1) will yield a scalar measure of the entropy as it evolves over time in the information channel representing the original Lagrangian model. The goal is to see what this time dependent entropy trace tells us about the actual Trajectory model as applied to its particular domain.

Conversion of Lagrangian Distributions to Eulerian Densities

At its most fundamental layer a Lagrangian distribution is defined as the coordinate positions of some collection of (N) particles. Without any loss of generality, the collection of all possible particle positions may be considered as bounded within some as of yet unspecified domain. The typical output from a Lagrangian model is graphically presented as a plot of particle locations, appearing somewhat like a swarm of bees. Or, if the model output is time dependent, it might be an animation of a series of these plots. Such displays are easy to interpret in a qualitative sense and useful in showing the

movement and spreading of particles representing the dependent variable distributions.

For a more quantitative evaluation of Lagrangian distributions, it is necessary to convert the model output to an Eulerian density field. To accomplish this, a generalized density is defined with dimensions of MASS/VOLUME. In a computational sense this amounts to assigning some measure on the spatial domain, that can be thought of as a "neighborhood" or "region of influence" to each of the Lagrangian particles and forming a ratio of the particle's mass with this measure. There are a variety of ways to approach this problem and they are not necessarily unique. Global constraints are required to ensure conservation of mass. In addition, some commonly used computational methods will result in aliasing the derived information channel entropy. This aliasing of the derived information will be discussed when it comes up in the analysis to follow.

The MASS portion of this density definition is associated with the Lagrangian point data and the VOLUME portion of the definition is associated with the model domain. It is important to understand that a generalized Eulerian transformation will require two separate mappings, or functions that operate on different sets. The MASS function operates on the Lagrangian point data and produces a non-negative scalar for each LE:

$$MASS|:(particle_i) \Rightarrow (m_i | m_i \geq 0 \wedge m_i = scalar) \tag{2}$$

The cardinality of the mass set is over index i which will span all of the Lagrangian particles, thus $(1 \leq i \leq N)\ where\ N = number\ of\ particles.$

The VOLUME function operates on the domain set which bounds the cumulative potential locations of all of the Lagrangian point data and also results in a non-negative scalar:

$$VOLUME|:(spatialdomain) \Rightarrow \left(v_j | v_j \geq 0 \wedge 0 \leq j \leq J \wedge v_j = scalar\right) \tag{3}$$

The cardinality of the volume set is over the index j and could be any integer value

greater than zero. When cardinality of the MASS set and the VOLUME set are equal $(i = j)$ a special case exists and this will have some influence on the potential information entropy of the model output as is explained below. It should also be apparent that the spatial domain on which the VOLUME mapping works may have a geophysical dimensionality of one, two or more but the result v_i must still always be a scalar.

Example of VOLUME Function

Example – of VOLUME functions based on tessellation

A Cartesian grid where the domain is partitioned into adjacent rectangular boxes is obviously an example where the cardinality of the v_i set has no relation to the cardinality of the m_i set and boxes may or may not be a proper partition of the spatial domain.

A partition of the spatial domain based on nearest neighbor to any location m_i of a MASS element can be used. This "neighborhood" approach yields a Delaunay triangulation (and its topological duo, Thessian polygons) with the cardinality of the MASS set equal to that of the VOLUME set and is a proper partition of the spatial domain. An example of this approach is given in Galt (2011).

Example – of VOLUME function based on kernel analysis

Cluster analysis where the VOLUME function yields a scalar metric that weights the clustering or separation distances found around any particular LE provides the cardinality of the MASS set equal to that of the VOLUME set, but does not in general represent a proper partition of the spatial domain. An example of this approach is given in Galt (2015).

Kernel methods which operate on the spatial data of the Lagrangian particles will typically be extensions or subsets of the cluster analysis method based on some assumed kernel function.

Generalized Density Function Requirements

Regardless of what VOLUME function is used, the generalized Eulerian density

function ρ_i is defined only after each member of the MASS set is associated with a single member of the VOLUME set:

$$Density(LE_i) = \rho_i = \sum_j \frac{m_i(v_j)}{v_j}$$
$$where \tag{4}$$
$$m_i(v_j) = m_i if(m_i \subset v_j)$$
$$m_i(v_j) = 0 if(m_i \not\subset v_j)$$

Any VOLUME element could be associated with zero or more MASS elements, but each MASS element is associated with a unique VOLUME element. Obviously there may be some j index values that do not contain any mass if the cardinality of the VOLUME set is greater than the cardinality of the particle set. These extraneous VOLUME elements will have no MASS associated with them and never contribute to the density field.

Finally, the transformation of Lagrangian point data to Eulerian density data has a global requirement that total Lagrangian mass must match the total Eulerian mass. Obviously it would not make physical sense if the transformation either created or lost material. This condition will be met if the association of $m_i \Rightarrow v_j$ is unique so that we have:

$$M = \sum_j \rho_i \, v_j \tag{5}$$

Where M is the total mass of the Lagrangian particles in the scenario.

Eulerian Density Fields Viewed as Probability Densities

The density field described in equation (3) defines the distribution of the total mass (M)

throughout the model domain in terms of the individual component masses of the Lagrangian elements (LEs) and their associated neighborhoods. By normalizing these by the sum of the neighborhood weighted densities, as shown in equation (4), we obtain the fraction probability of mass associated with each LE to the total mass:

$$probability(P_j) = \frac{\rho_i \nu_i}{\sum_j \rho_j \nu_j} \tag{6}$$

The P_j values represent the spatial distribution of mass as forecast by the trajectory model and have the proper mathematical form for a probability, that is, all values are greater than or equal to zero and the sum of all the probabilities over the index i for all LEs or over index j for all the spatial measures is unity.

$$\sum_i P_i = \sum_j P_j = 1 \tag{7}$$

Extending the summation over j contains no additional probability information since volume elements that do not contain any mass will automatically have zero probability. However, inclusion of these values may make a difference in the model information channel's base entropy, which will be defined in the following sections of this study.

Simple Information Channel Cases

Nearly all of the important facets of a Lagrangian trajectory model's behavior, as viewed through its information channel, can be demonstrated with a few very simple cases. The simplicity of these cases makes the computational aspects easy to follow, while at the same time revealing the profound connections between the dynamic behavior of the model and the entropy variations and uncertainty elucidated in its information channel. Figure (1) indicates seven panels, each of which shows an instantaneous view of the output from a simple Lagrangian trajectory model, including the LE MASS positions

and VOLUME boundaries. In each case the LEs have unit MASS and the total model domain is also unity. The seven cases (panels a thru g) are walked through their mathematical computations to obtain their associated information channel. Then the channel's entropy is discussed with reference to what it means about the behavior of the Lagrangian Trajectory model.

Case (a)

The interpretation of these results are straightforward.

$$N(numberofparticles) = 1$$
$$J(numberofvolumes) = 1$$
$$MASSm_1 = 1$$
$$VOLUMEv_1 = 1$$
$$EulerianDensity(eq4)\rho_1 = 1$$
$$Probability(eq6)P_1 = 1$$
$$Entropy(eq1)E = 0$$
$$EntropyBase\big(ln_2(J)\big) = 0$$

The entropy (E) is zero, meaning that the model completely specifies the location of the Lagrangian elements. In this case there is only one particle mass (m_1) and there is no question about its location, that is there is only one VOLUME (v_1) where it could be. Zero entropy implies no uncertainty. The entropy base is also zero which implies that no matter how the mass particle moves around the domain it will always result in zero entropy or no uncertainty. There is always only one VOLUME or address where it could be found. The information channel representing this very simple Lagrangian model will never degrade over time given this set up.

Case (b)

We now move on to the Lagrangian trajectory model with output as seen in panel (b). This is very similar to the output shown in case (a) except that the model domain is partitioned into two different regions, $(v_1 and\ v_2)$. Applying the appropriate calculations

$$N(numberofparticles) = 1$$
$$J(numberofvolumes) = 2$$
$$MASSm_1 = 0, m_2 = 1$$
$$VOLUMEv_1 = 0.5 v_2 = 0.5$$
$$EulerianDensity(eq4)\rho_1 = 0 \rho_2 = 2$$
$$Probability(eq6)P_1 = 0 P_2 = 1$$
$$Entropy(eq1)E = 0$$
$$EntropyBase\big(ln_2(J)\big) = 1$$

Looking at these results shows that once again the Lagrangian trajectory model for case (b) yields an information channel with zero entropy. This is because all of the Lagrangian mass particles are found within a single VOLUME. There is no uncertainty about where the model's mass is found. The base entropy, unlike case (a) is not zero, but rather one. The entropy could go up. This means that as the model continues to evolve it might be possible for the Lagrangian particle to wander into the presently empty second VOLUME partition. Statistically speaking over a period of time the mass particle might be found in the right or left side of the domain. The information needed to distinguish this right/left choice is one binary bit. To state this in another way, if the total Lagrangian mass was equally divided between all the specified VOLUME elements then each LE would require one additional binary bit of metadata, which was not specified by the Lagrangian trajectory model and thus represents uncertainty.

Thinking this through we see there are some potential problems. First, there is only one mass particle, and the density mapping function requires that each mass element must be associated with a unique VOLUME element. This condition will be violated if we try and associate parts of a mass particle to more than one VOLUME. In case (b) the only available particle will always be in either the right or left VOLUME and the entropy will always be zero. The entropy base becomes meaningless, because it can never be realized. The second problem is that the cardinality of the VOLUME space is set by whoever is carrying out the Eulerian transformation and it does not necessarily have anything to do with the actual Lagrangian trajectory model. It is common for an analyst to place a Cartesian grid over the model output and estimate Eulerian densities by counting LEs in each rectangle. This is a bad choice, because the answer will depend on

the grid size and (as in this case) if $J > N$ the entropy maximum case will not represent a realizable state. **It should be taken as a general rule that any Eulerian density transformation procedure should restrict itself to cases where $J = N$.**

Case (c)

The Lagrangian trajectory model output shown in panel (c) represents a modification of panel (b) by the simple expedient of adding one more LE so that the condition $J = N$is satisfied. Applying the appropriate calculations:

$$N(numberofparticles) = 2$$
$$J(numberofvolumes) = 2$$
$$MASSm_1 = 0, m_2 = 2$$
$$VOLUMEv_1 = 0.5v_2 = 0.5$$
$$EulerianDensity(eq4)\rho_1 = 0\rho_2 = 4$$
$$Probability(eq6)P_1 = 0P_2 = 1$$
$$Entropy(eq1)E = 0$$
$$EntropyBase\big(ln_2(J)\big) = 1$$

As in the previous case, the information channel representation of the Lagrangian trajectory model has an entropy of zero, since all of the mass particles are associated with a single VOLUME element. In this case however the evolution of LEs moving around within the domain could lead to a realizable uniform Eulerian density distribution. (One mass particle in each VOLUME segment.) This case demonstrates that if for some computation reason it is necessary for there to be a fixed number of VOLUME elements, the consistency requirement $J = N$ can be obtained by going back and reformulating the Lagrangian trajectory model such that the cardinality of the particle set matches that of the VOLUME set.

Theoretically any situation where:$(J = \alpha N | \alpha = integer > 0)$, will also give a realizable entropy base state. In practice if N is a large number and $(J - N) \approx 0$ the approach to the entropy base state should be acceptable. Stated another way, if a plot of the Eulerian density vs. VOLUME elements appears to be a constant then the entropy base state has been effectively reached.

Case (d) and Case (e)

Up to this point the concept of a Lagrangian trajectory model evolving over time has been mentioned, but left vague. We will now be a bit more specific. Cases (d) & (e) depict instantaneous output of a Lagrangian trajectory model, but they are the same model shown at two different times. Case (d) depicts the initial conditions and case (e) is the same model's output after a long time (essentially infinity). From this, we can see the information channel view for the initial and final state of a typical Lagrangian trajectory model.

Case (d) shows a Lagrangian trajectory model representation of a domain that is partitioned into two sections. All of the LEs are located in the right hand side. Applying the appropriate calculations:

$$N(numberofparticles) = 10$$
$$J(numberofvolumes) = 2$$
$$MASSm_1 = 0, m_2 = 10$$
$$VOLUMEv_1 = 0.5 v_2 = 0.5$$
$$EulerianDensity(eq4)\rho_1 = 0\ \rho_2 = 20$$
$$Probability(eq6)P_1 = 0 P_2 = 1$$
$$Entropy(eq1)E = 0$$
$$EntropyBase\big(ln_2(J)\big) = 1$$

Once again the entropy in the information channel view of this model is zero, because all of the MASS particles are in a single VOLUME element. At this point it is useful to observe that many Trajectory models of pollutant discharges take as initial conditions that the particles to be tracked are originally in a single location (for example, a tank or an accidental release point) and these will always have an initial relative entropy of zero. This initial entropy will always be relative to some final entropy base, which depends on the cardinality of the VOLUME set, and in this case is one. The difference between the entropy and the entropy base is a measure (in bits of metadata) of the information that the model provides compared to a hypothetical model on the same domain, that provides no information about the statistical placement of LEs. With this in mind we now consider the next case which will represent the same model, but after a long time has elapsed.

After an assumed long time the model in the previous panel evolves into the representation shown in case (e). This is characterized by the MASS particles being uniformly spread out over the entire domain. Applying the appropriate calculations:

$$N(numberofparticles) = 10$$
$$J(numberofvolumes) = 2$$
$$MASSm_1 = 5, m_2 = 5$$
$$VOLUMEv_1 = 0.5v_2 = 0.5$$
$$EulerianDensity(eq4)\rho_1 = \rho_2 = 10$$
$$Probability(eq6)P_1 = P_2 = 0.5$$
$$Entropy(eq1)E = 1$$
$$EntropyBase\big(ln_2(J)\big) = 1$$

From these results it is seen that the information channel's view of the model has an entropy of one, which is the same as the entropy base. This is equivalent to the statement that the model provides no statistical information about where in the domain a particular LE is located and an additional bit of metadata (right/left) would be required with each LE to completely determine its location.

The panels in the last two cases present a figure that should be familiar to anyone who has had an introduction to thermodynamics. For example, if panel (d) represented a volume divided in half such that the right hand side contained a number of molecules at a particular temperature (T) with the left hand side a vacuum and at a later time panel (e) represents the same system after the divider has been removed (subject to the condition that no energy exchange takes place with the outside world) then the molecules have dispersed throughout the entire domain in an adiabatic process and the temperature has gone down, as well as the chemical entropy. Taking the limit as the left hand volume approaches infinity the temperature will approach absolute zero. Just as the 2nd law of thermodynamics and conservation of energy lead to the concept of chemical entropy in a physical domain, the probability density and its distribution leads to the concept of information entropy in a communication channel. This analogy was of course understood by Shannon and his choice of relating uncertainty in information content to "information entropy" makes perfect sense.

Now let's consider this analogy in terms of Lagrangian trajectory modeling. Most

natural geophysical fluid domains (oceans, lakes, streams or the atmosphere) are dispersive. We start with a collection of floating objects that are initially contained at a single location and are released into the marine environment (for example: an oil spill, flotsam from a tsunami, etc). At the point of release they have a reference entropy of zero (all of the LEs are in a single VOLUME). Once the LEs are released, they move and spread out (their entropy increases) and, as time increases, their position becomes more and more uncertain. Ultimately, if the dispersion continues, the LEs will be spread over the entire domain. At this point the probability density distribution is flat and the information channel is at its entropy base. This base state depends only on the cardinality of the domain and has nothing to do with the initial condition of the spill, such as where it took place. At that point the original information in the model is completely lost.

In a geophysical model diffusion, non-linear advection, chaos, and wind interactions all contribute to dispersive processes. They are usually important and at some scale dominate the trajectory movement. For these cases information entropy will start at zero when the model time equals "spill time" and increase towards a value equal to the entropy base. The derivative of the entropy with time is positive and its magnitude indicates the extent to which it is losing the ability to statistically distinguish particle position. This leads to the first basic rule of information entropy as derived from a trajectory model. **Model dispersive processes drive the information channel entropy up, and lead to less specificity in the determination of LE locations**.

Case (f) and Case (g)

We will now go on to a different Lagrangian trajectory model where there is no diffusion and the VOLUME set follows a "nearest neighbor" rule based on particle MASS positions. The domain will again be a unit square with a weak uniform current across the left hand boundary and a weak uniform current across the bottom. The upper and right hand boundaries are blocked so the water level is slowly rising, but we will only model horizontal movement.

These cases show views of Lagrangian trajectory model output separated by time, but in this case displaying very different behavior as seen from the information channel view.

These two panel pairs will isolate and demonstrate the second fundamental evolutionary behaviors expected in the information channel entropy representation of a Lagrangian trajectory model.

The initial model output is shown in panel (f). These initial conditions have 4 symmetrically placed particles, each of which is surrounded by a nearest neighbor region. Applying the appropriate calculations:

$$N(numberofparticles) = 4$$
$$J(numberofvolumes) = 4$$
$$MASSm_1 = m_2 = m_3 = m_4 = 1$$
$$VOLUMEv_1 = v_2 = v_3 = v_4 = 0.25$$
$$EulerianDensity(eq4)\rho_1 = \rho_2 = \rho_3 = \rho_4 = 4$$
$$Probability(eq6)P_1 = P_2 = P_3 = P_4 = 0.25$$
$$Entropy(eq1)E = 2$$
$$EntropyBase\big(ln_2(J)\big) = 2$$

We see that the probability distribution is uniform and the entropy is 2. The entropy base is also 2 meaning that this particle distribution started off well dispersed. From an information channel point of view 2 bits of position metadata (up/down, right/left) would be needed to completely specify particle locations. We, of course, contrived this initial condition and strange current system to demonstrate a point.

Panel (g) shows the model results for panel (f) after a short time where the horizontal currents represent a convergence towards the upper right corner of the domain and crowds the floating particles in that direction. Applying the appropriate calculations:

$$N(numberofparticles) = 4$$
$$J(numberofvolumes) = 4$$
$$MASSm_1 = m_2 = m_3 = m_4 = 1$$
$$VOLUMEv_1 = 0.1111v_2 = v_3 = 0.2222v_4 = 0.4444$$
$$EulerianDensity(eq4)\rho_1 = 9.0\rho_2 = \rho_3 = 4.5\rho_4 = 2.25$$
$$Probability(eq6)P_1 = 0.1111P_2 = P_3 = 0.2222P_4 = 0.4444$$
$$Entropy(eq1)E = 1.836$$
$$EntropyBase\big(ln_2(J)\big) = 2$$

These results show that the entropy has gone down (0.136 bits) relative to its initial state. This is due to the clustering effect of a convergent current system. In real geophysical flow fields there are often convergent phenomenon in surface currents associated with baroclinic fronts, internal waves, variable depth, tidal rips, Lagrangian coherent structures, beaching, etc. The list goes on and on. In this demonstration case we assumed no dispersion so that the clustering dominates. This leads to the second basic rule of information entropy as derived from a trajectory model. **Model clustering processes drive the information channel entropy down, and lead to more specificity in the determination of LE locations**.

Generalized Non-dimensional Entropy Graph

In a real situation there will usually be a dominant dispersive effect modified by smaller scale or occasional cluster effects. What the time dependent entropy in a model's information channel shows is some mix of their opposing processes. This will define the time scale at which a model's initial information content loses its relevance and when new data must be assimilated to maintain its usefulness.

When applying this understanding to oil spill trajectory models it is worthwhile to note that dispersive processes spread the spill out, add to its positional uncertainty, and degrade the ability of the model to forecast just where it might go. On the other hand, clustering processes tend to move the pollutant together, increasing probability of encountering it in some particular region. Virtually all spill response countermeasures depend on high encounter rates. An understanding of the balance between dispersive and clustering processes in a spill trajectory model is a very desirable feature.

The cases that have been considered so far have provided a generic understanding of the behavior that we expect a Lagrangian trajectory model to display in its information channel entropy. Envision a normalized rectangular graph with time going along the horizontal axis starting at zero on its left hand edge and entropy along the vertical axis ranging from 0 along the lower edge. Since the maximum possible entropy is $\left(ln_2(j)\right)$ it makes sense to form a non-dimensional measure of entropy as $entropy/\left(ln_2(j)\right)$. This means all possible values of non-dimensional entropy can be plotted on the vertical axis between 0 and 1. In general the initial conditions of the model will yield relatively low

or zero starting values of entropy, so the entropy vs. time curve will start in the lower left hand corner of the graph. If diffusive processes are scaled as a random walk with a displacement step $(\delta)$for each model step interval, while the model is characterized by a length scale L a useful non-dimensional time scale is:

$$T_0 = (L^2/4\,\delta^2) \tag{8}$$

This will then typically mean information channel entropy times will plot along the horizontal axis a distance of order 1.

Based on this scaling a typical non-dimensional entropy plot is shown in figure (2). Various regions of this graph are annotated. The entropy curve traces to the right over time and typically, under the influence of dispersive processes, will rise towards the entropy base limit. At some point the curve approaches this upper boundary indicating the model's degradation in usefulness and the need for data assimilation. For geophysically realistic domains the entropy curve, while trending up, may show considerable small scale changes in slope, rising more sharply when dispersive processes become more dominant and flattening out or even going negative in cases where clustering processes dominate. The vertical resolution of the graph will depend only on the cardinality of the VOLUME elements used in the Eulerian density transformation. While most entropy vs. time curves will show normalized traces similar to figure (2) details will be totally controlled by the localized movement and spreading processes within the Lagrangian trajectory model that is being examined. In a real sense it will be a scalar signature or fingerprint of the model. Embedded in it is a great deal of time scale information on spreading, clustering and relative information content. The next section of this study will consider these time dependent signals in more detail.

Numerical Studies

Here we consider Lagrangian trajectory models which represent an idealized rectangular domain on a geophysical scale which has a realistic number of particles and are subject to a set of well-defined physical processes. We start by considering a square domain on a Cartesian grid with sides of length 10^7micro degrees. In geophysical terms this would

represent a 10 degree by 10 degree square on the equator (a square approximately 600 nm on each side). All of the models considered in this section will include basic dispersion which is isotropic in two dimensions. This will provide a non-dimensionalization using L (the width or height of the domain in $microdegrees$) and k (kinematic diffusion in $microdegrees^2/sec$). Following a random walk implementation for diffusion and scaling suggested by Csanady (1973) we define the random step size for $\delta t = 1sec$ as $\delta_0 = 2k\delta t$. From this we may choose a time scale equal to $T_0 = L^2/4\,k$which, related to the time in seconds, it would take for the random walk displacements to add up to a trip half way across the model domain. All model output will be shown in non-dimensional time t/T_0. For the following studies the model will be run for 1000 steps out to a non-dimensional time of unity and the random walk step size will be corrected from the one second step size by $\delta = \delta_0\sqrt{10^{-3}T_0}$.

Study of pure diffusive scale

In this section we will introduce a more detailed Lagrangian trajectory model which exhibits purely diffusive behavior. In this model the only physical process will be diffusion represented by a random walk, which is characterized by a step length. The model will be initialized with 1024 LEs placed in the center of the domain. The expectation is that the Lagrangian model's information channel will start with zero entropy and transition toward a final state with a theoretical maximum entropy of 10 bits/particle.

The theoretical entropy maximum of 10 will of course only take place if the probability distribution is actually flat. Random distributions resulting from diffusion will only obtain this value as an infinite ensemble collection of random end states. For any single diffusive end point the theoretical value will fall short of this because all of the VOLUME elements are not quite the same size. In order to get an understanding of what is expected by a single model run to a random end state a test was made with an initial random distribution of the original 1024 particles. One of these random end states is shown in figure (3). As can be seen the spacing of the particles are more or less uniform, but the nearest neighbor VOLUME elements are not exactly uniform. The entropy calculations done on a number of tests of this scenario produced a mean non-

dimensional value of 0.93 with a standard deviation of less the 0.01. This then defines the "degradation band" suggested in the upper part of figure (2). At this point the Lagrangian trajectory diffusion model is run for a thousand steps. This amounts to about 1.0 of the suggested non-dimensional time. At first we examine the tessellation of the LE particle distributions at various intervals. A number of these are shown in figure (4). The first panel of this figure shows the results at non-dimensional time 0.05. The particles have diffused a short distance from their initial central position. The entropy is increasing. The nearest neighbor of most of the LEs is still small and only the outer fringe of particles are associated with low densities. The second panel shows the results after non-dimensional time 0.1. The diffusive effects operating on the initial cluster are more evident. The central panel shows the model results after non-dimensional time 0.3. The LEs have now spread over the central region of the domain and clearly the largest areas of VOLUME calculated via the nearest neighbor routines are diminishing rapidly. The lower left hand panel shows the results after non-dimensional time 0.6. Now the LEs are scattered over most of the domain, but there is still obviously a central tendency. The diffusive process has not yet given a uniform appearance and lost all of the initial location information, but it is definitely approaching that limit. The final panel in the lower right hand side of the figure shows the dispersion at non-dimensional time 1.0. This shows virtually all of the central tendency is lost and we are very nearly to the state shown in figure (3). Figure (4) just shows the standard Lagrangian trajectory model scatter plot of particles with a tessellation based Delaunay triangularization (Galt, 2011).

To carry on the analysis and formulate an information channel view for this Lagrangian trajectory model it is necessary to calculate the Eulerian density associated with each of the particles. The nearest neighbor VOLUME elements for each particle are associated with the Voronoi diagram (Thessian polygons), which is the topological duo of the Delaunay triangles (Galt, 2011). To examine the density distribution data for this model the values are calculated and sorted from minimum to maximum for the cases shown in Figure (4). These results are shown in figure (5). This graph shows that initial density values have a very sharp increase at the high end of the distribution (relative to the mean value). As time increases and diffusive (anti-clustering) processes continue the maximum values drop quickly. Then as time increases these highest values tend to

asymptote towards a flat, or uniform distribution indicating that it is approaching an entropy maximum state.

Finally, from the distributions of density it is possible to define probability fields. These in turn can be used in Shannon's equation to calculate a normalized entropy trace similar to what is anticipated in figure (2). Figure (6) shows the results of an ensemble of 10 cases which are run for a Lagrangian trajectory model initialized at a central point. The lower panel in the figure is an overlay of the ten scenarios.

They all start at an initial zero entropy and after a non-dimensional time approaches unity trend towards the limit of 0.92. The upper panel shows the mean and standard deviation of the ten traces in the lower panel. Individual scenario traces show some variation which causes slight deviations from a smooth evolution of the entropy vs. time curve, but these variations are seen to decrease as the number of steps increase, as would be expected in any random process.

With the non-dimensional scaling that was introduced, any changes in the number of particles used in the model or in the diffusion coefficient are absorbed into the (0-1.0) range of the axes shown in figure (6). The vertical range is normalized by $\left(ln_2(LEs)\right)$and the horizontal range by $T_0 = L^2/4\,k$so variations in these parameters plot to the same universal curve (Figure 7). This was checked by repeating the numerical experiment over a range of inputs and was shown to be true.

Study of mixed convergence/diffusive scale

The diffusive Lagrangian trajectory model described in the previous section is now extended to include a clustering component. This is accomplished by adding a convergent velocity field represented by the current pattern shown in figure (8). This pattern shows velocities that are everywhere directed towards a central Latitude line. The speeds are zero at the North and South boundaries of the domain and linearly increase to unity at the central Latitude. The actual velocities used in the model will be determined by a scaling speed constant $\alpha_v(length/time)$ which will be referred to as the convergence coefficient. To make this non-dimensional we simply express the α_v length scale in terms of δ the random diffusion step size. This non-dimensionally links

the convergence process relative to the diffusive process. For example with $\alpha_v = 0.1$, convergence velocities near the central part of the model would sweep LEs a distance one tenth of the distance of a diffusive random step towards the centerline during each model step. The geophysical result will be to inhibit their movement away from the central band (clustering).

Analysis of single convergence zone

This model set up representing a convergence zone, or Lagrangian coherent structure will be investigated by considering two different initial states. The first will be with the LEs initialized as a point source in the center of the model, and the second will be with the LEs initialized as a random distribution over the whole domain. In the first case we start with all the LEs located at the exact center of the convergence region in a very low entropy state and, as the model evolves, we see the entropy drift upward as particles escape the zone of the Lagrangian coherent structure. In the second case we assume that a convergence appears in a high entropy state of highly dispersed LEs and, as the model evolves, we expect the entropy to decrease as clustering takes place and the convergence, or Lagrangian coherent structure, captures particles. The end state of either of these cases should trend to a steady final entropy where the statistical diffusion of LEs escaping the Lagrangian coherent structure is just equal to the number that are captured by its convergence.

Both cases of this numerical experiment are run with a convergence coefficient $\alpha_v = 0.1$. For each case an ensemble of 10 runs was included and the results are shown in figure (9). In many respects the upper two panels, representing the point source case, look similar to what is shown in figure (6) for the pure diffusion case. The major difference, however, is that the end state does not approach the random state limit of 0.93 but a reduced entropy limit closer to 0.65. This difference is the clustering drop in entropy caused by the convergence. The lower two panels of figure (9) represent the case initialized by a random distribution of LEs. In this case the entropy starts out at the expected maximum (0.93) and declines towards a final value close to 0.65 approaching the same limit as seen in the first case. The final state in either case seems to be nearly independent of the initial conditions and for constant normalized geophysical processes is controlled only by the diffusive and advective balance into and out of the

convergence.

Variations in convergence strength

In order to test this diffusion/convergence balance, cases were run for α_v values set at 0.05, 0.1 and 0.2 initialized by point source and random conditions. A summary of end states at $T_0$is shown in figure (10).

In the upper panels with a convergence coefficient of 0.05 it is seen on the left that many LEs have escaped the central convergence and are diffusing over the entire region. On the right the central convergence is collecting (clustering) particles, but not strongly enough to strip the entire domain. For both cases however the distribution is dominated by the loosely clustered central collection of particles and the information channel entropy is approaching a constant value of 0.83. The central panels represent a convergence coefficient of 0.1 and their entropy evolution is shown in figure (9) approaching a limit value of 0.65. The lower panels show a convergence coefficient of 0.2 where the convergence processes clearly dominates the diffusive processes. On the left virtually none of the LEs are escaping the central convergence region. On the right nearly all of the LEs have been swept into the central structure. The distribution is dominated by the strongly clustered central collection of particles and the limiting entropy value in the information channel representation approaches 0.50.

Rate of change of entropy

There are several other features of the information channel representation of a Lagrangian model with clustering that are worthy of note. First, it is apparent from the lower panels of figure (9) that the initial decrease in entropy from a random state occurs at a nearly constant rate. A little study also shows that for different values of convergence coefficient (α_v) this remains a constant. However, the slope (rate of change of entropy) changes depending on the actual value of α_v. Figure (11) shows a plot of the normalized rate of entropy change for variations in the convergence coefficient. The superimposed red curve shows that the actual rate of entropy loss is linearly related to the convergence coefficient. In addition, the zero intercept $(\alpha_v = 0)$ is positive. In the absence of convergence this is the (virtual) uniform dispersive increase that the convergence (clustering) is working against. **This suggests a practical and heuristic**

method of quantitatively measuring the strength of a Lagrangian coherent structure. 1) Initialize a number of LEs randomly distributed over the structure. 2) Let the model evolve in time and measure the initial normalized rate of decrease in entropy. This will be a quantitative measure of the strength of the structure's clustering power.

Study of diffusive and beaching scale

It is common that Lagrangian trajectory models include processes that allow for particles to come in contact with shorelines where they are subject to a different set of algorithmic behavior representing beaching, stranding, re-floating, etc. The question is how to represent the information channel entropy when this happens. The answer to this question is to recognize that the "floating" particles and "beached" particles are represented by two different sets. The probability densities of these separate sets may depend on different VOLUME functions because the representation of the "floating" domain is generally not the same as the "beaching" domain, and in fact will usually have different dimensions. Floating densities will be $(mass/length^2)$ and beaching densities will be $(mass/length)$. Details about how to merge these sets together for a generalized Lagrangian trajectory model are documented in the appendix of this study.

At a basic level, a Lagrangian trajectory model, which includes beaching, will have a Shannon entropy equation (replacing equation 1):

$$Entropy = E(t) = -\frac{F_n}{N}\sum_{i\in F} p_i \, ln_2 p_i + \frac{B_n}{N}\sum_{i\in B} p_i \, ln_2 p_i \qquad (9)$$

This is just seen to be the individual entropy of all of the particles in the "floating" subset weighted by the fraction of floating particles plus the individual entropy of all the "beached" particles weighted by the fraction of beached particles.

As a simple check we see that if all of the particles are floating then equation (9) reduces to equation (1). Also if all of the particles are beached the entropy is simply based on

their entropy and no "floating" processes are represented. It is also obvious from equation (9) that if the probability density values are all equal and are completely in either set the entropy max will be $ln_2 N$ as in previous examples. If, on the other hand, some of the particles are floating and some are beached, and in both sets the probability densities are "locally" flat, the entropy max will be reduced to as much as $0.5ln_2\, N/2 + 0.5ln_2\, N/2 = (ln_2 N - 1)$. It may seem strange that beaching the particles statistically reduces the maximum theoretical entropy by up to exactly one bit. The answer to this apparent question becomes clear when we recall that the information channel entropy indicates the uncertainty in particle position (or metadata) that is **not** provided by the Lagrangian trajectory model. In this case the model has provided data (floating/beached) which represents at least the potential of one bit of information that will not show up in the information channel entropy calculation.

In order to carry out numerical studies with beaching we need to modify the model that has been used in the previous examples. In the earlier models there were no boundaries and any particles that moved beyond the model domain simply reappeared by entering through the opposite side. In essence the model domain represented a view of an infinite cyclic repeating space. For this study, any particles that exit the model domain will be: 1) held at the exit location and 2) moved from the F (floating) set to the B (beached) set. The Eulerian density calculation will use tessellation with Thessian polygons (Galt, 2011) for the F set and cluster analysis (Galt, 2015) for the B set. Once the Eulerian densities have been defined, probabilities can be calculated and information channel entropy obtained from equation (9).

Beaching from a uniform random distribution

The first beaching case we will consider is a Lagrangian model initialized with N = 1024 random particles uniformly distributed over the domain. The only geophysical process included is random-walk diffusion so that as particles near a boundary are displaced outside the domain they are more or less randomly appearing in the B set and thinning out the edge concentrations in the F set. Views from this numerical experiment are shown in figure (12).

The upper panel of figure (12) shows the output from the Lagrangian trajectory model

with the red triangular mesh indicating the triangular tessellation of the F (floating) set after the model has run for a period of time. Surrounding the floating particles are the beached particles in black. The thinning out of floating particles along the boundaries can be seen so that the actual rate of transfer from floating to beaching will go down over time.

The central panel shows the time dependent development of a number of the model's computational components for one trial run. Note that the time axis extends to 2 T_0, or twice the non-dimensional time. This is because the beaching time scale is not well defined in terms of diffusive processes and we want to make sure to illustrate asymptotic effects. The curves in this panel are for one case study and show 1) fraction of floating particles, 2) fraction of beached particles, 3) the entropy contribution calculated for the floating particles, 4) the entropy contribution calculated for the beached particles, and 5) the weighted sum of the entropy as derived from equation (9). Initially 100% of the particles are floating and the total entropy is dominated by the F set. By non-dimensional time of approximately 0.6, over half of the particles are beached and the entropy is dominated by the contribution of the B set.

The third panel shows the mean total entropy (equation 9) of 10 case studies and their standard deviation. This panel shows the initial entropy starting at about 0.93 which is what the expected value for all of the particles floating and randomly distributed. The value falls quickly for two reasons. First of all the particles immediately start to beach, which shifts them from the F set to the B set. Secondly, as the particles are removed from the bands along the boundary, clustering effects are introduced into the floating particle density and probability structures. The net result is that the total normalized entropy drop is about 0.2. This is about twice what we would expect due to just partitioning the particles into two sets.

Beaching from a point source

The next numerical scenario to investigate is based on the same set up that was used in the previous example, except that the Lagrangian trajectories are initialized at a single point in the center of the domain. The data from these runs are summarized in figure (13). The upper panel of this figure shows the output from a Lagrangian trajectory as

the central cluster of particles has started to diffuse far enough so that beaching occurs first along the mid-range of each of the four sides of the model. Beached particle locations are shown in black around the edge of the panel and the internal triangular structure connects the floating particles in red.

The central panel shows the time dependent development of a number of the model's computational components for one trial run. Note that the time axis extends to 2 T_0, or twice the non-dimensional time. The curves in this panel are for one case study and show 1) fraction of floating particles, 2) fraction of beached particles, 3) the entropy contribution calculated for the floating particles, 4) the entropy contribution calculated for the beached particles, and 5) the weighted sum of the entropy as derived from equation(9). Initially 100% of the particles are floating and the total entropy is dominated by the F set. In this case the floating particles, which are initially at a maximum distance from all the boundaries, take some time to even start beaching. In fact it is non-dimensional time of nearly 1.9 before half of the particles are beached. Initially both the floating particles entropy and beached particles entropy are zero. The floating particles entropy being zero because all the particles are in the same place, and the beached particles entropy is zero because it is a null set. When the models diffusive processes first start to transfer a few particles into the B set the beached entropy is erratic because the sample size is quite small. As more particles beach it continues to grow and smooths out. Initially the total entropy is dominated by the large fraction of floating particles, as time goes on and more particles beach the total entropy clearly moves towards an intermediate mix of the two components.

The third panel shows the mean total entropy (equation 9) of 10 case studies and their standard deviation. This panel shows the initial entropy starting at about 0.0. The value rises quickly and peaks as the particles first start to beach. As the beaching set starts to grow its probability densities are decidedly non-uniform. The net result is the total normalized entropy drops from a maximum of about 0.8 to about 0.76.

It is interesting to note that the final limits of the total entropy for this study and the previous one are both approaching non-dimensional values of around 0.75. Comparing the upper panels of figure (12) and (13) we see that they appear somewhat similar,

although the probability distributions are not uniform in slightly different ways.

Beaching with strong asymmetry from advection

The third set of scenarios that we will consider while investigating beaching will all be initialized as a point source of 1024 particles placed in the center of the geophysical domain. The particles will be subject to a random walk simulating diffusion and a constant current, or advection in the easterly direction. As the initial concentration diffuses and spreads (increases entropy) the entire group will move towards the down current shoreline and start beaching but, unlike the previous case, virtually all of the beached particles will show up in the B set as tightly clustered in a reduced entropy state. The data from these runs are summarized in figure (14). The first panel shows the geophysical output from the Lagrangian trajectory model at some time after the initial point source has diffused and has been advected by the current towards the eastern boundary of the model. The red triangle mesh shows the locations of the floating particles and the black points indicate the beached particles. It is obvious that the beaching process is clustering particles along the center of the eastern shoreline. From this we will expect that the entropy of the B set will be lower than we have seen in the more random (less clustered) cases.

The central panel in figure (14) shows the time dependent trace for a case of floating particles, beached particles, entropy of the F set, entropy of the B set, and the total information channel entropy. These all reflect the fact that the floating particles experience beaching more rapidly than the previous cases studied since the current is sweeping them towards the boundary. In addition, as the beaching becomes active both the floating and beached distributions become non-uniform and both exhibit clustering and a subsequent decrease in entropy.

The third panel of figure (14) shows the mean and standard deviation of an ensemble of ten cases. Initially the entropy rises quickly as the point source disperses. It peaks at non-dimensional values of 0.7 at non-dimensional time 0.35. At this point, it starts to fall due to localized beaching and the clustering of floating particles in the eastern region of the model. Ultimately most of the particles end up in the B set, concentrated in one segment of the model domain. This final configuration has a total entropy of about 0.43

reflecting the mostly beached set of particles.

This completes the studies of a geophysical Lagrangian trajectory model and its information channel representation. We have shown how model processes such as diffusion, convergence/divergence zones and beaching all are reflected in the entropy representation of the model. Up to this point all the studies have focused on the entire model domain. We now move on to consider the localization of entropy change for a sub region of the model domain and trace this metric as it follows a particular Lagrangian particle.

Global vs. local Entropy change

An important feature to notice about any particular Lagrangian convergent model process as viewed from an information channel becomes obvious when the entropy computation spans the entire model domain and particles are conserved. If we start out from a maximum entropy state, convergence results in clustering and the total entropy goes down. On the other hand if we start out at the maximum entropy state, and localize a divergence (dispersive) process it will spread out the particles, but that will just mean that they cluster somewhere else. Once again the entropy goes down. Figure (15) shows the results of two Lagrangian model runs at time $T_0$where the convergence coefficient is equal to 0.1 and -0.1. In the upper panel we see the convergence is collecting particles in the center of the domain and the resulting clustering drives the entropy down. In the lower panel we see the divergence thinning out particles in the central region, but that just causes them to bunch up or cluster along the upper and lower boundaries and again drives the entropy down. A check on the initial rate of entropy decrease for these cases shows them to be the same.

In most of the cases where we carry out information channel analysis on a trajectory model it will desirable to distinguish between a global and local view of the entropy. In particular we will be interested in the changes in entropy following a particular Lagrangian trajectory, rather than the global change over the entire conservative model

domain. With this in mind we need to focus on a specific method or algorithm to calculate the change in the information channel representation of a small patch or ensemble of Lagrangian particles localized in a small sub-region of the global model.

Entropy change related to generalized kinematic flows

To begin this localization study we may note all fluid flow fields can be decomposed using differential analysis (Yuan, 1967) into the following form:

$$\vec{V} = \overrightarrow{V_0} + \frac{1}{2}\left(\overrightarrow{\Omega \times dr}\right) + D \tag{10}$$

We will restrict our focus to 2 dimensional surface flows as is appropriate for Lagrangian trajectory models of floating pollutants. $\overrightarrow{V_O}$ is a uniform translation in the horizontal; $\frac{1}{2}\left(\overrightarrow{\Omega \times dr}\right)$ is a solid body rotation in the horizontal plane; and, D is the vertical component of the rate of strain, or rate of deformation tensor. We now introduce a number of randomly distributed Lagrangian particles into this perfectly general 2-dimensional flow and track their movement for a short interval. Calculating the information channel entropy at the beginning and end of the interval would show that the first two components of the flow (translation and rotation) will never introduce any change in the entropy. Any change in the information channel entropy view for this flow will be associated with the deformation tensor, and only with that component. This, of course, makes sense because any simple translation or rotation will not cause distributed particles to change the amount of the surrounding domain with which they are associated (their VOLUME function equation will not change). This means that their probability density field will not change and by Shannon's equation entropy will be constant. On the other hand the deformation tensor warps the surface area that the particles are floating on and this will change the probability densities of some particles relative to others and the initial local “maximum” entropy value will go down. **This is the fundamental relationship between Lagrangian trajectory models of floating pollutants and entropy as seen in their information channel representation.**

Localized general Eulerian differential motion

Equation (10) applies to any hydrodynamic velocity field. We will now consider restricting this to 2-dimensional surface movement and extend it to include all the factors acting on Lagrangian particles. For example, wind drift and retardation associated with beaching. If we define the movement field as $(u = xmovement, v = ymovement)$ then the movement field surrounding a point $V_0 = u_0, v_0$can be written as a Taylor series expansion:

$$v(\delta x, \delta y) = V_0 + \frac{\partial u}{\partial x}\delta x + \frac{\partial u}{\partial y}\delta y + \frac{\partial v}{\partial x}\delta x + \frac{\partial v}{\partial y}\delta y \tag{11}$$

And defining the horizontal component of the divergence as T:

$$T = \left(\frac{\partial u}{\partial x} + \frac{\partial v}{\partial y}\right) \tag{12}$$

The terms in equation (11) can be rearranged into a format similar to the vector form shown in equation (10), but now it applies to actual Lagrangian particle displacements, not just currents.

$$\begin{aligned} v(\delta x, \delta y) = Vo \begin{vmatrix} 1 & 0 \\ 0 & 1 \end{vmatrix} \begin{vmatrix} \delta x \\ \delta y \end{vmatrix} + \begin{vmatrix} 0 & \left(\frac{\partial u}{\partial y} - \frac{\partial v}{\partial x}\right) \\ -\left(\frac{\partial u}{\partial y} - \frac{\partial v}{\partial x}\right) & 0 \end{vmatrix} \begin{vmatrix} \delta x \\ \delta y \end{vmatrix} \\ + \begin{vmatrix} T & 0 \\ 0 & T \end{vmatrix} \begin{vmatrix} \delta x \\ \delta y \end{vmatrix} + \begin{vmatrix} \left(T - \frac{\partial v}{\partial y}\right) & \left(\frac{\partial u}{\partial y} + \frac{\partial v}{\partial x}\right) \\ \left(\frac{\partial u}{\partial y} + \frac{\partial v}{\partial x}\right) & \left(T - \frac{\partial u}{\partial x}\right) \end{vmatrix} \begin{vmatrix} \delta x \\ \delta y \end{vmatrix} \end{aligned} \tag{13}$$

Each of the matrix terms in equation (13) represent a uniform first order differential

component of all possible motions around a point and are pictured in figure (16).

The first two matrix terms of equation (13) shown in figure (16) represent simple translation and solid body rotation and, as such, will never introduce any changes in the information entropy representation of particles in the Lagrangian model. The second two matrix terms of equation (13) shown in figure (16) represent a further decomposition of the deformation tensor shown in equation (10) and will certainly cause local changes in the entropy representation of the trajectory model. These last two matrix terms will also have a clear geophysical interpretation in the Lagrangian trajectory model.

To understand these two matrix terms consider a small circular subset (area A) of the model domain surrounding a test point. Within this circular subset we will randomly distribute a fixed number of test particles (N). The entropy of this set up will be:

$$Entropy = \frac{A}{U} ln_2(N) \tag{14}$$

Where clearly A will be equal to the area interior to the convex hull of the N points and U is the global area of the entire model domain. As this collection of particles moves under the influence of a uniform divergence or convergence (third matrix term in equation (13)) all of the internal distances between particles within the convex hull will be uniformly scaled so the collection's internal entropy from Shannon's equation will remain the same. On the other hand, the total area of the convex hull surrounding the collection will change so the area (A) in equation (14) will change. Now consider this same test collection moving under the influence of uniform hyperbolic deformation (fourth matrix term of equation (13)). In this case the various distances between particles interior to the collection will change from the initial value of $ln_2(N)$ to some value representing the cluster of the hyperbolic deformation.

The behavior of this small test collection of particles embedded in a Lagrangian trajectory model gives a local, point specific measure of the entropy change reflected in

the model's information channel representation. This is seen as a sum of two terms: The first representing the external change of the convex hull and the second due to the internal rearrangement of particles.

Algorithmic heuristic measurement of entropy change following an individual trajectory

Algorithm Development

From the discussion in the previous section, we are able to define a standard algorithmic approach for calculating the change in information entropy following an individual particle trajectory in any particular Lagrangian model. It is assumed that these calculations are made as a post processor to a standard trajectory run and that at each forecast interval the location of any particle is available. In addition, it is assumed that the model can be re-run with all of the movement fields reproduced (deterministically or statistically) as in the original run. The setup and definitions used are outlined in figure (17).

For any interval in the model's evolution a start location for the particle is determined as $P1$ and the position of that same particle at the next forecast interval is identified as $P2$. Half of the distance between $P1$and $P2$is defined as $R1$. A circular test region of radius $R1$ centered on location $P1$ is created and populated with N randomly placed particles. For this collection of particles two calculations are made. First, the total area interior to the convex hull is assigned to $A0$ and, secondly, the entropy based on a tessellation of the convex hull is assigned to $E1$. The test collection of particles is then run forward through a duplicate hindcast of the Lagrangian trajectory model to the forecast end point. For the modified collection of test particles the convex hull and entropy calculations are repeated as $A0 + dA$ and $E2$.

With these four data values we can return to equation (13) and identify the local external change in entropy due to pure convergent or divergent processes acting on the total collection is calculated by introducing a uniform stretching of the Cartesian domain:

$$\begin{aligned} A0 &\rightarrow A0 + \delta A \\ p_i &\rightarrow \left(\frac{A0}{A0 + \delta A0}\right) p_i \\ \Delta A_i &\rightarrow \left(\frac{A0 + \delta A0}{A0}\right) \Delta A_i \end{aligned} \tag{15}$$

Substituting these into following form of the Entropy equation:

$$E_{expand} = -\sum \left(\frac{A0}{A0 + \delta A0}\right) p_i ln_2 \left(\left(\frac{A0}{A0 + \delta A0}\right) p_i\right) \left(\frac{A0 + \delta A0}{A0}\right) \Delta A_i \tag{16}$$

Which reduces to:

$$E_{expand} = ln_2 \left(\frac{A0}{A0 + \delta A0}\right) - E \tag{17}$$

$$\delta E_x = E_{expand} - E = ln_2 \left(\frac{A0}{A0 + \delta A0}\right) \tag{18}$$

And the local internal changes in entropy due to rearrangement of particles within the collection:

$$\delta E_i = E2 - E1 \tag{19}$$

This gives a total change in entropy along the trajectory during a forecast period as:

$$\delta E = ln_2\left(\frac{A0}{A0 + \delta A0}\right) + E2 - E1 \quad (20)$$

Repeating this test over a sequence of forecast periods will yield the cumulative change in entropy following an individual particle throughout the model evolution influenced by the geophysical process within the neighborhood of the actual trajectory path. Particles following different paths will show different changes in entropy reflecting different degrees of uncertainty. For example trajectories moving through, or into strong convergence structures would tend to show less entropy increases, or uncertainty, relative to trajectories not encountering such structures. An experienced trajectory analyst who has worked with models that resolve strong tidal rips (Cook Inlet - spills off Kenai, Ak) or coastal estuarine fronts (Gulf coastal areas – Atchafalaya and Mississippi outflow, i.e., Alvenus spill off Lake Calcasieu, LA) will have recognized this sort of behavior, but without entropy analysis it is very difficult to put a quantitative measure on the uncertainty of the results.

In some respects this simple algorithm can be thought of as a **Numerical Entropy Change Meter (NECM)** . It can computationally be associated with any Lagrangian particle of a properly configured trajectory model. The post processor will then estimate the information channel entropy change (uncertainty) for that particular particle pathway. Applying this to a number of particle trajectories over the model domain will indicate the relative strength of the forecast in its various sub-regions and suggest where and when data assimilation would be helpful.

*Interpretation of **NECM** change information.*

In previous sections of this study there were numerous references to the changes of information entropy for an entire modeling domain. When the entropy values were normalized against ln_2(Num_of_LEs) it was demonstrated that as the model progressed from an initial zero entropy state and approached a value of one it generally lost its resolving power and approached a random distribution of particles. The **NECM** does

not operate on the entire model domain so we must modify our interpretation of changes in entropy. For the cases we are going to investigate, the model has an output time step of six hours so that the domain over which the information entropy change is calculated is a circular region moving along the trajectory path with a diameter of this six hour travel distance. After this six hour period the **NECM** algorithm resets the entropy values and initializes a new step. Because the entropy change associated with each step is independent the cumulative change in entropy does not have a limit. A non-dimensional value of plus one only means that an LEs position has become uncertain with respect to the six-hour domain it is associated with. Net negative changes in entropy values over a **NECM** calculation step mean that uncertainty in particle position is not going up due to the fact that internal deformation is compressing the probability distribution faster than the external dispersive processes are spreading them apart. In order to evaluate the relative strength or voracity of a trajectory we will take a conservative approach and consider net positive changes of entropy for each computational step as cumulative and net negative entropy changes as simply delaying any increase in entropy (or uncertainty) over the period of that time step. In this way changes in total entropy will always be zero or positive and when cumulative values approach a non-dimensional value of one it will indicate that the model predictions are uncertain within the area of a **NECM** computation in time and space. That is on the order of +/- three hours and about a radius of 10 kilometers for the cases to be studied.

Case Study – Aleutian Trajectory Model

To demonstrate the application of the Numerical Entropy Change Meter (NECM) we will focus on a version of the Navy's HYCOM circulation model configured for the Northern Pacific and Bering Sea. This model was incorporated into the NOAA trajectory model (GNOME) and forced using a reanalysis of three years of wind data. This work was initially done by the NOAA Marine Debris Program to study the distribution of flotsam from the Japanese tsunami of March 2011. This is typical of the many large-eddy-simulation models that are available for use in modern particle trajectory formulations. The techniques shown here could be used in any such model.

We will concentrate on three trajectories that are initiated at the same location and are

tracked for a seven day period. Each of these trajectories starts at a different time and represents a different point in the ocean-atmosphere situation space. Each example moves through a different region in the model and is subject to different time-dependent wind and current fields. Each could be thought of as an individual attempt at simulating a trajectory for a real time forecast.

The three single particle trajectories are shown in figure (18). For each of the trajectories the circular cluster of test particles is shown for successive 6 hour periods. The size of the test cluster is governed by the displacement of the trajectory over the time step (in this case 6 hours) and typically has a radius of about 10 kilometers, but varies from step to step and trajectory to trajectory. Each test cluster is inserted into the model and its initial area A1 and entropy E1 are calculated. Then the model is run forward and its final area A2 and entropy E2 are calculated. These values are then inserted into the algorithm outlined above to calculate the change in entropy for the time step.

Bering Sea Trajectory

The first trajectory under study is the one which moves generally westward into the Bering Sea. Figure (19) shows the incremental components of the entropy change (blue – external caused by convergence or divergence of the cluster) and internal (red – caused by deformation with the cluster) where the values have been normalized to $\ln_2(1024)$. Looking at the external components (blue) we see that the external, or expansion terms are consistently positive. These add to the overall entropy along the trajectory and confirm that the model is dispersive. Uncertainty increases. A spike in the entropy at the beginning of day 6 appears to be associated with the slow down and reversal of the trajectory. The internal deformation induced change in entropy (red) is generally smaller and represents convergences or divergences internal to the test cluster of particles. From figure (11) we note that these values are close to linear representation of the strength of the local convergence or divergence. Another important way to look at the entropy change data is to consider the cumulative sum of entropy change over the span of the trajectory. This curve is obtained by adding the net positive components of

entropy change from each interval over successive intervals. As was explained previously in this paper; when the non-dimensional entropy increases to about unity the predictive power of the model degrades towards the point where predictions are not significantly different from random. In this case we mean random with respect to the size of the test cluster, which implies plus or minus 3 hours and over an area of radius of approximately 10 kilometers. For anyone accustomed to oil spill reconnaissance overflights this is approximately the view available from an overflight at 1000 feet. Figure (20) shows the cumulative change in entropy curve for Track 1 as well as the cumulative entropy on the assumption that assimilation data was available to reinitialize the model (set entropy to zero) at intervals defined by raw normalized cumulative entropy approaching unity. Looking at the trajectories in figure (18) we see that to maintain confidence in the trajectory forecast an infusion or assimilation of new data would be required after about four days. If done correctly this would reset the cumulative entropy curve to zero and the forecast could continue for approximately two more days before the dispersive nature of the physical processes in the model would again require data assimilation. This technique of checking the strength of a trajectory forecast at run time is a unique feature of this analysis.

Bering Shelf Trajectory

The second trajectory under study is the one which moves generally Northward and then onto the Bering Shelf. Figure (21) shows the incremental components of the entropy change (blue – external caused by convergence or divergence of the cluster) and internal (red – caused by deformation within the cluster) where the values have been normalized to $\ln_2(1024)$. Its general characteristics are similar to Track 1, but it also shows some significant and interesting differences. As in the previous track the external components are uniformly positive indicating that the model is predominately dispersive, and the internal deformations are quantitatively smaller and more variable. A striking difference in this track is that the entropy changes in the first two days of the trajectory are very different from what is seen in the next five days. The entropy changes in the initial period are nearly twice the magnitude of the values in the remaining time span. Referring to figure (18) the initial two days of Track 2 are when the trajectory moves

across the edge, and into the wake of, strong Northerly currents from Unimak Pass. The HYCOM model obviously resolves some of this complexity as non-linear eddies which show up in the divergence and deformation fields and thus show up as signals in the entropy change. Another indication of model complexity as the trajectory comes out of the Unimak Pass wake into the more quiescent region is what appears to be harmonic signals in the internal entropy (red). Figure (22) is a repeat of figure (21) with two different series of internal entropy peaks marked. These are presumably convergent bands in Lagrangian structures encountered as the trajectory moves parallel to and then across the Bering Shelf. The temporal steps in the analysis are not fine enough to say much more, but it should be pointed out that these signals are related to the local physical processes within the model and provide details that are not part of the typical trajectory analysis suite. In addition, anyone who has worked in modeling oil spills for real response operations knows that the location of convergence process are critical to forecasting regions of "high encounter rates" needed for recovery processes.

It is also important to consider the cumulative net entropy change along the path taken by Track 2. Figure (23) shows this curve. Like the previous track this curve has a continuous positive slope and over the seven day run gains about the same maximum value, but it differs in that there is a significant break in the slope at about two and a half days presumably because of the Unimak Pass wake effect. As before we can redraw this as a hypothetical curve assuming the timely data assimilation which is also shone in figure (23). In this case the normalized entropy limit is reached at 2 days and 3.25 days so that the forecast trajectory degenerates quite rapidly during the first half of its travel.

Unimak Pass Trajectory

The third trajectory in the set we investigate using **NECM** methods is significantly different than the previous examples for two major reasons. First, it quickly moves into the very complex dynamics of Unimak Pass and, secondly, the trajectories cause a significant number of the LEs to beach. During its first day this trajectory moves into the rapidly accelerating intake of currents flowing South through the Pass. As the LEs accelerate they are extended and drawn into bands, or filaments. These strong

convergences show up as negative components of entropy change. In addition to this process, particles that encounter shoreline will beach and this version of the model does not allow for re-floating. Beaching basically acts as a type of convergence. The beached particles will still contribute to the overall entropy as described in the appendix of this report and equation (9). However, the total probabilities of floating and beached particles generally leads to a reduced entropy and beached particles will never contribute to an external (divergent) increase in the local entropy. Both of these factors contribute to an entropy distribution that is initially dominated by net negative increments. Figure (24) shows the incremental components of the entropy change (blue – external caused by convergence or divergence of the cluster) and internal (red – caused by deformation within the cluster) where the values have been normalized to $\ln_2(1024)$. During the first third to half of this trajectory the models deformation processes dominate and the overall dispersive nature of the model is suppressed, indicating lower entropy build and less uncertainty. Figure (25) shows the cumulative entropy gain following this trajectory and a hypothetical curve assuming the timely data assimilation. In this case, the normalized entropy limit is reached only after 4 days and then the forecast trajectory degenerates quite rapidly after several additional assimilations over the next couple days.

Conclusion

The goal of this study was to conduct a new type of analysis on the particle distribution data produced as time-dependent output of a trajectory model. The first step in this process is to calculate an Eulerian density field which may then be used to formulate a density probability field. This portion of the study utilized tessellation methods that have been fully described in previous reports of this series.

The second step in the analysis covers new material and is based on considering the density probability field as a communication channel. Using classical methods of information theory the information channel entropy for the Lagrangian particle model is calculated. It is shown that the time dependent evolution of the entropy characterizes the physical processes that occur within the model.

Generalized development of density probability fields are described. Calculation of information channel entropy is demonstrated using simple geometric domains and regional partitions. Non-dimensional scaling provides a way to set objective base levels for evaluating entropy change. Expected changes in entropy due to mixing, spreading, Lagrangian structures within the underlying trajectory model formulation are documented using simplified numerical experiments.

Finally, the information channel entropy methods are applied to three individual trajectories of an ocean-scale large-eddy simulation Lagrangian particle model (HYCOM). Differential components of entropy change are calculated and related to physical processes within the model. In addition, it is possible to identify (in real time for the model forecast) the build up of uncertainty within the model simulation and identify when data assimilation will be necessary to restore simulation integrity.

For this study, the primary application used information theory and entropy analysis for floating pollutants. However, this approach is clearly extensible to other types of model applications. In particular, one could introduce Lagrangian particles in a hydrodynamic model as a quality check on when the model would benefit from new data or when/where the model convergence/divergence areas appear. LEs could also be used to represent particles other than pollution, for example oyster larvae, marine debris or atmospheric particles (if one was using an air dispersion model).

References

Csanady, G. T. (1973) Turbulent Diffusion in the Environment . D. Reidel Publishing Co. Boston, MA. pp248.

Galt, J. A. (2011) 11-001 Triangle Tessellation Documentation. www.genwest.com/Publications Genwest Technical Publications.

Galt, J. A. (2015) 15-001 Triangle Tessellation Documentation Part II. www.genwest.com/Publications Genwest Technical Publications.

Pierce, John R. (1961) An Introduction to Information Theory – Symbols, Signals and Noise Second, Revised Edition. Dover Publications, Inc. New York, NY. pp305

Roman, Steven (1997) Introduction to Coding and Information Theory. Springer, New York, NY. Pp323

Shannon, Claude E. and Warren Weaver (1963) The Mathematical Theory of Communication. Univ. of Illinois Press, Urbana and Chicago, Il. pp125

Yuan, S. W. (1967) Foundations of Fluid Mechanics. Prentice-Hall, In. Englewood Cliffs, NJ. pp608.

Figure 1. Simple Lagrangian Trajectory Models for analysis as information channels

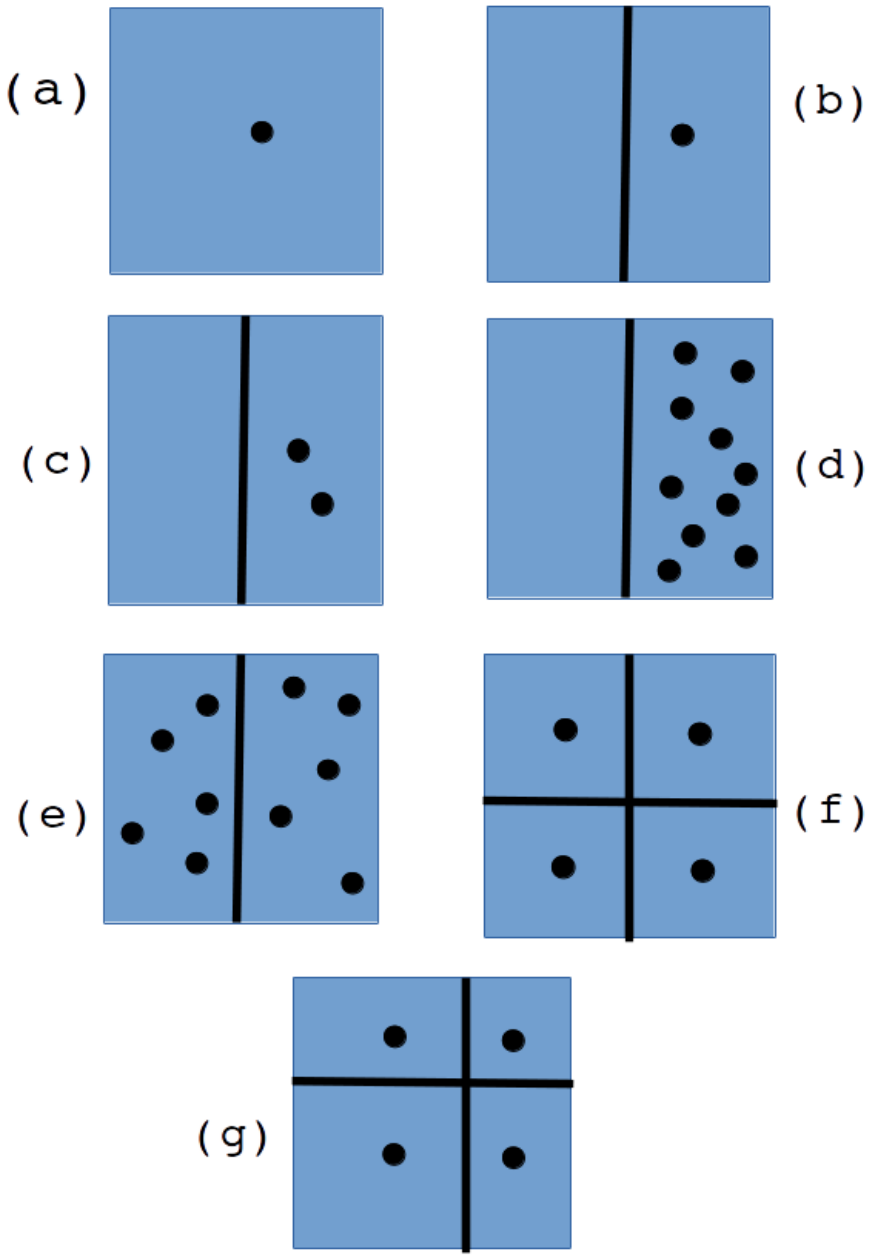

Figure 2. Generic graph of entropy vs. time as seen in the information channel representation of a Lagrangian trajectory model

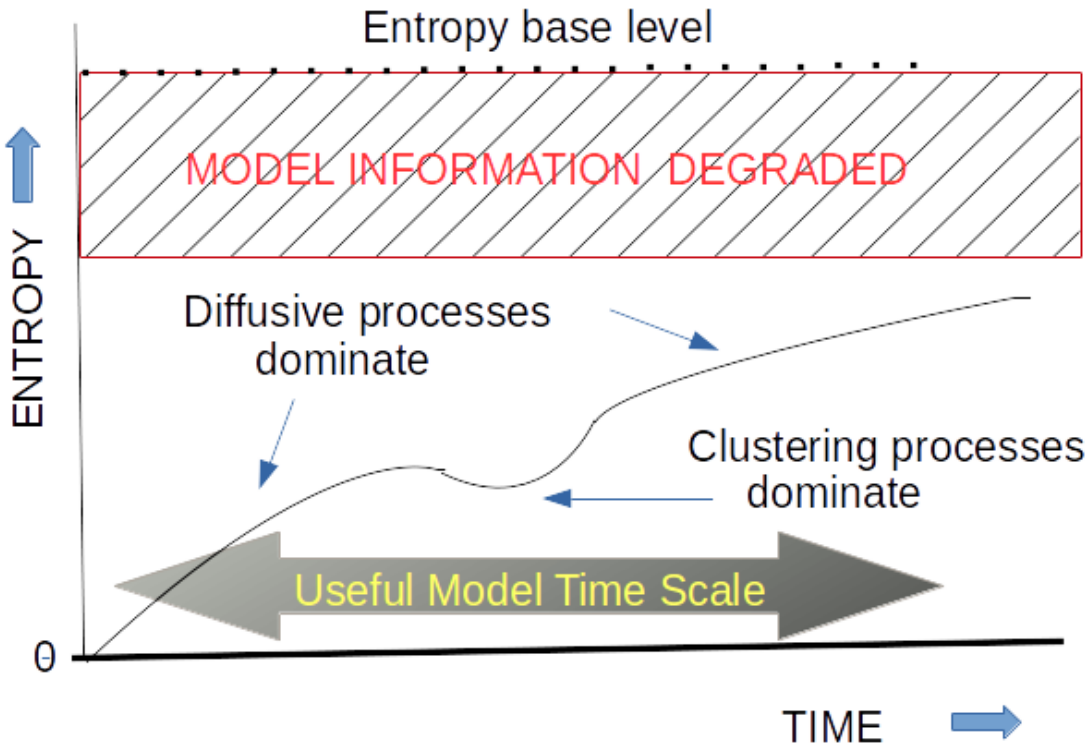

Figure 3. The mesh generated from a random placement of 1024 Lagrangian particles

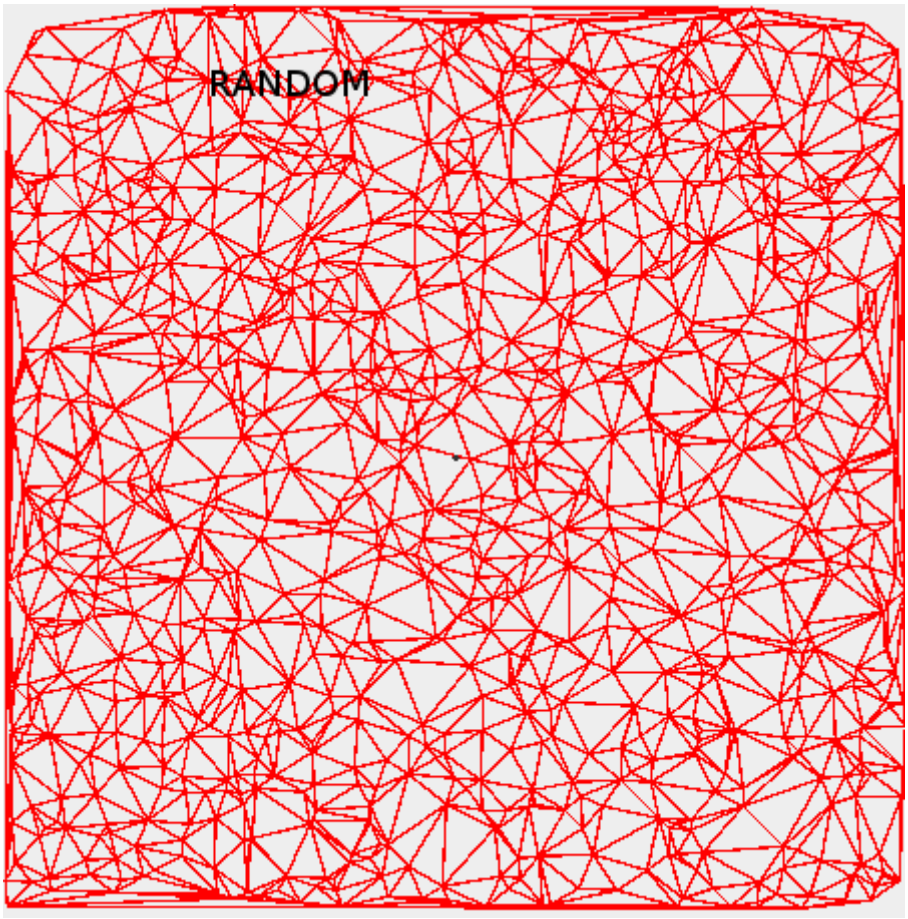

Figure 4. Plots of Lagrangian trajectory diffusion model for various non-dimensional times

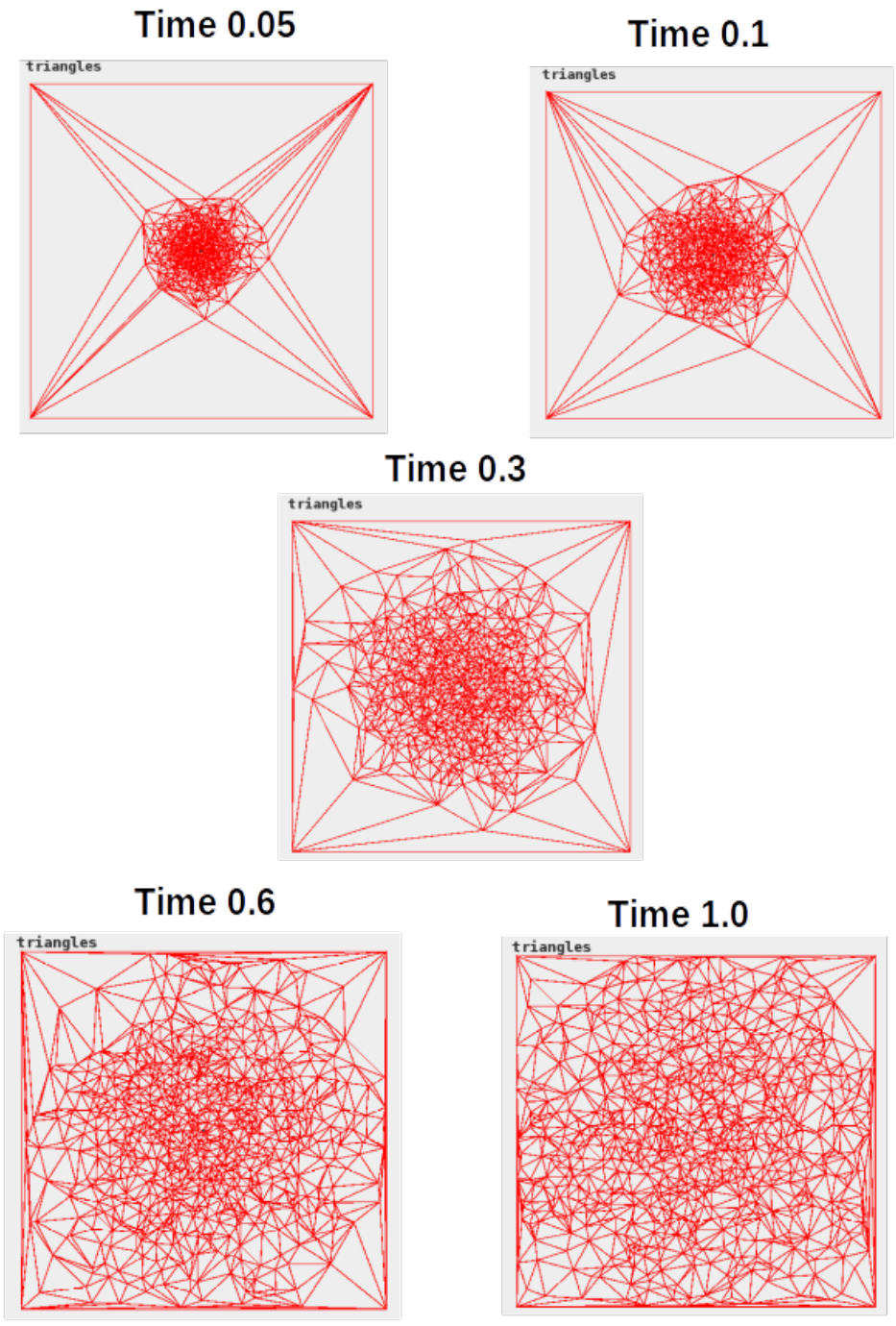

Figure 5. Sorted density distributions for the model times shown in figure (4)

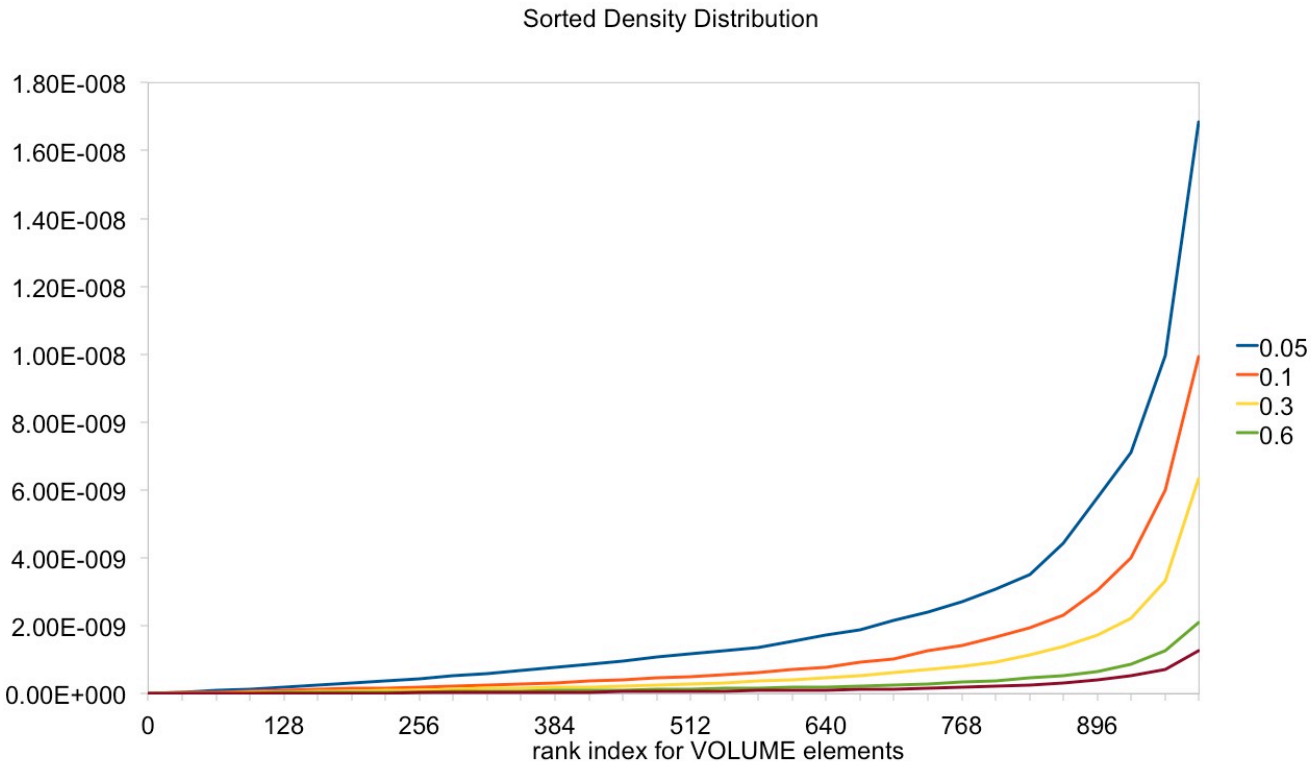

Figure 6. Ensemble Entropy example shown in non- dimensional form

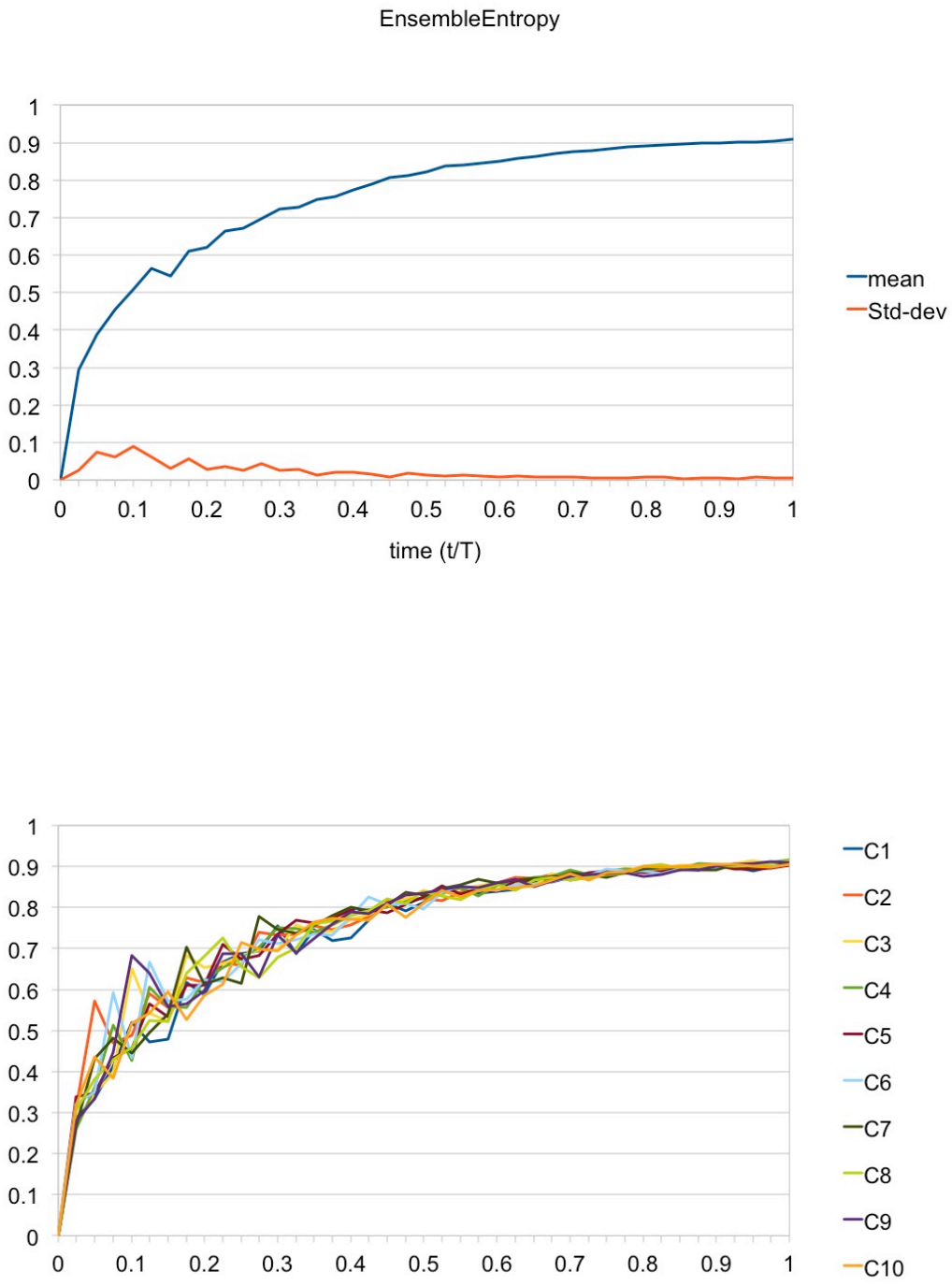

Figure 7. Ensemble Entropy traces overlay for variations in scaling parameters

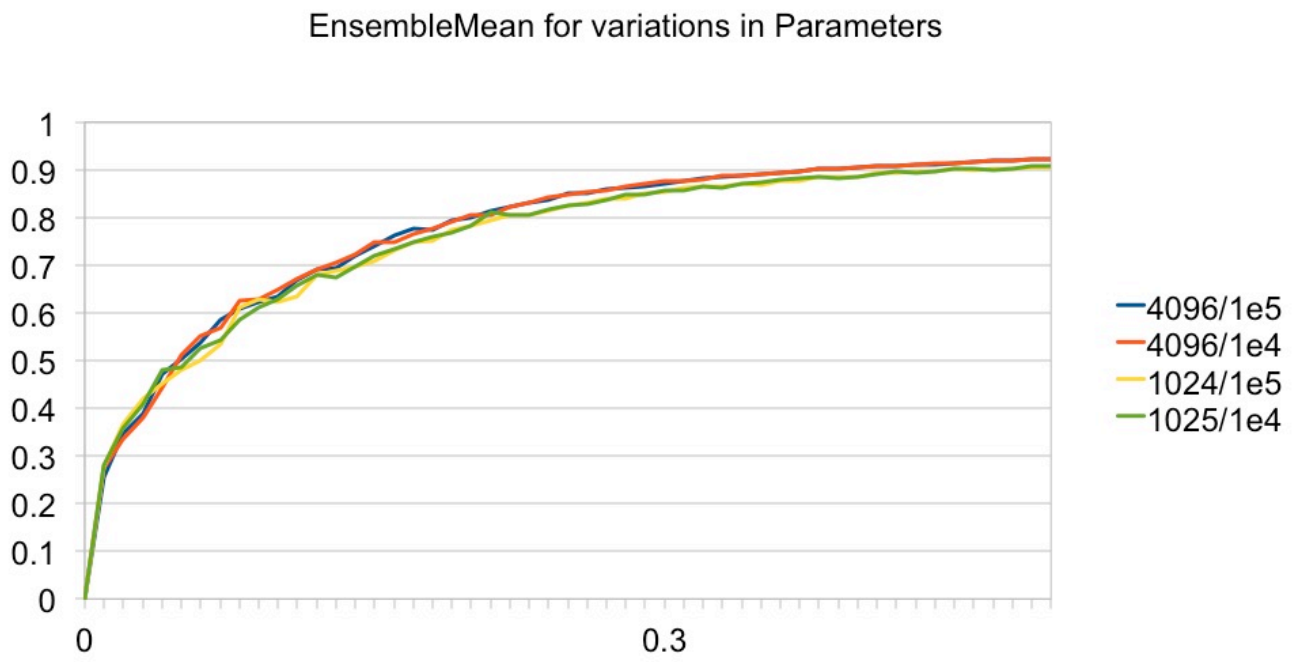

Figure 8. Current pattern showing line sink representing a convergence zone, or Lagrangian Coherent Structure

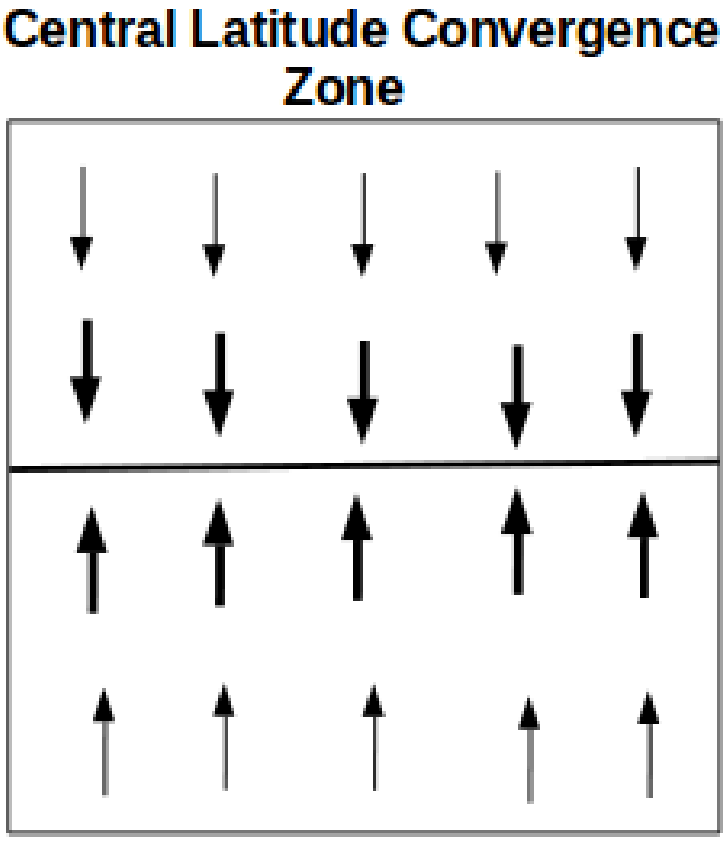

Figure 9. Test results for convergence cases with the convergence coefficient set to $\alpha_v = 0.1$. Upper panels show results for initial source as central point source. Lower panels show results for initial source as a random distribution

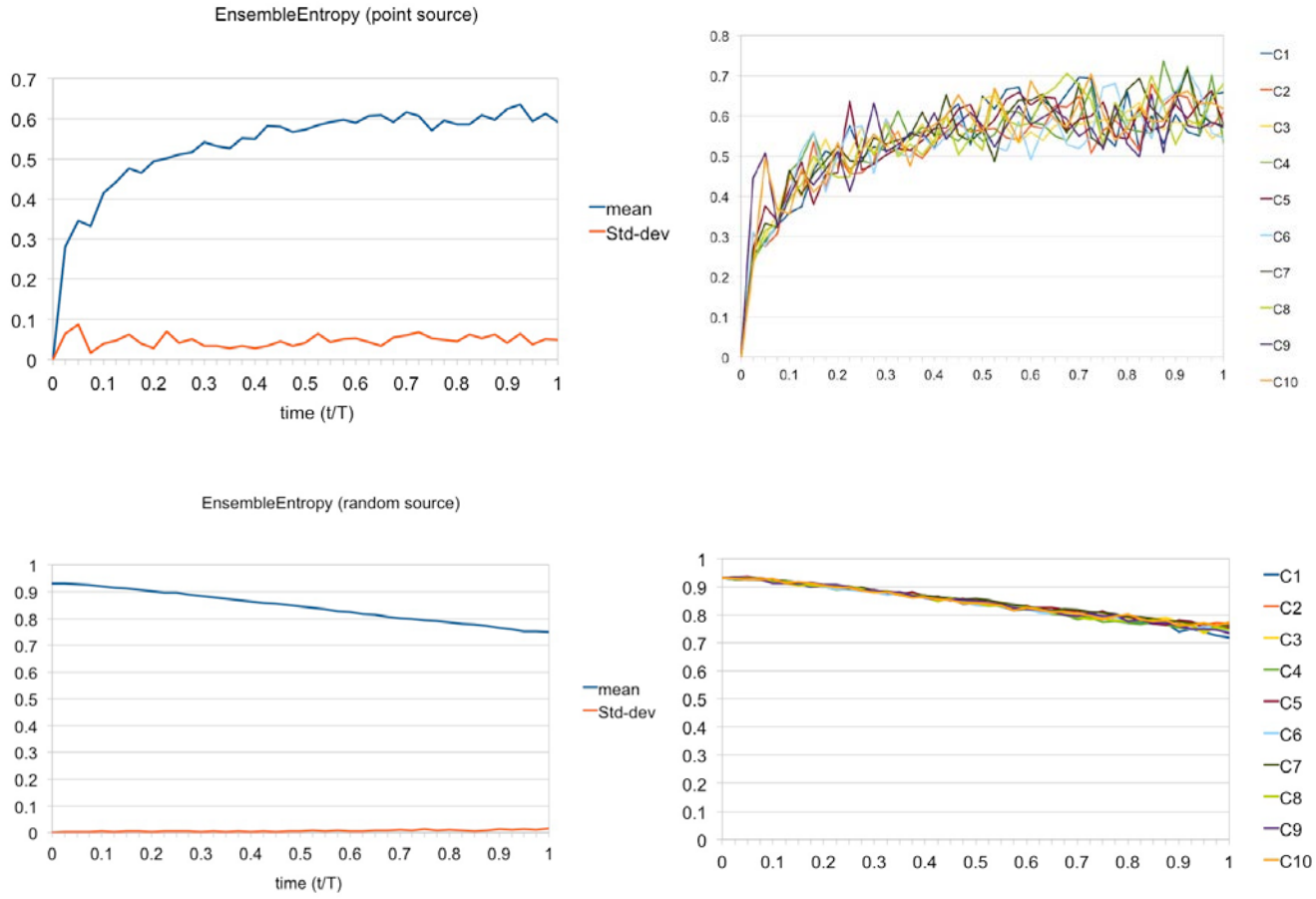

Figure 10. LE particle distribution shown for time T_0 for different convergence coefficient values. Left panels show results initialized from a point source. Right panels show results initialized from a random distribution

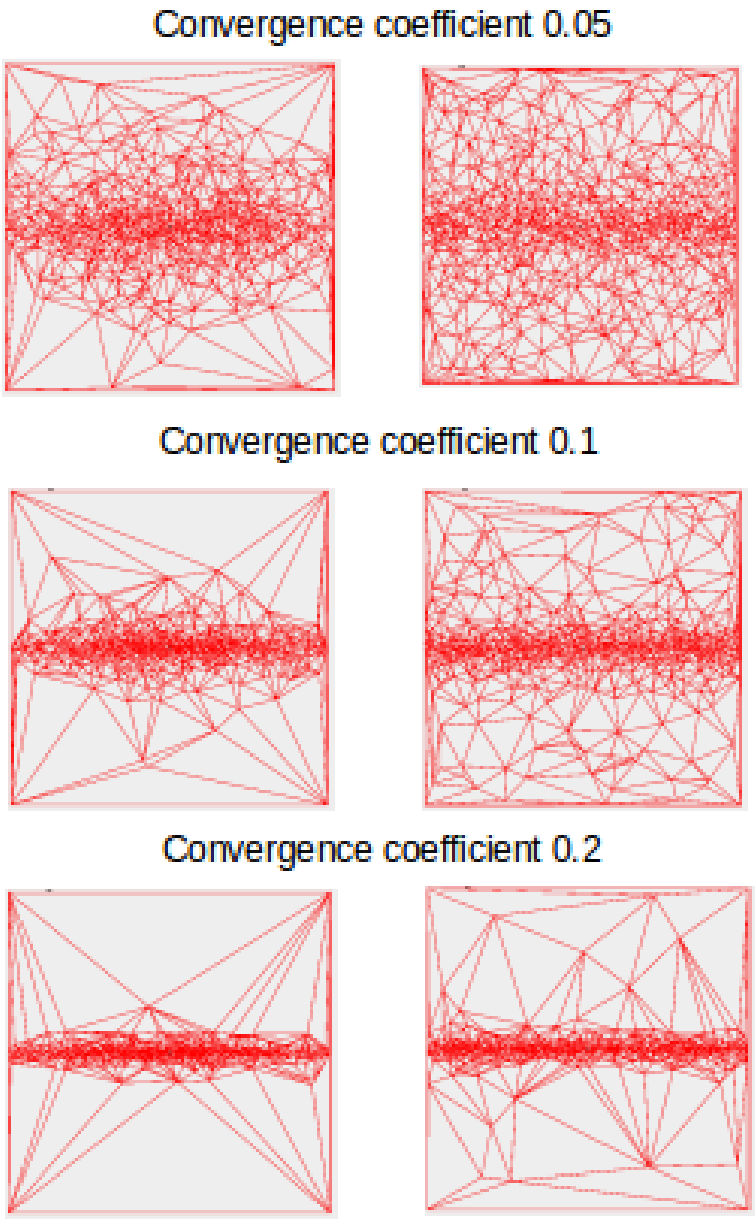

Figure 11. Graph of the initial normalized rate of entropy change from a random state for various values of convergence coefficient

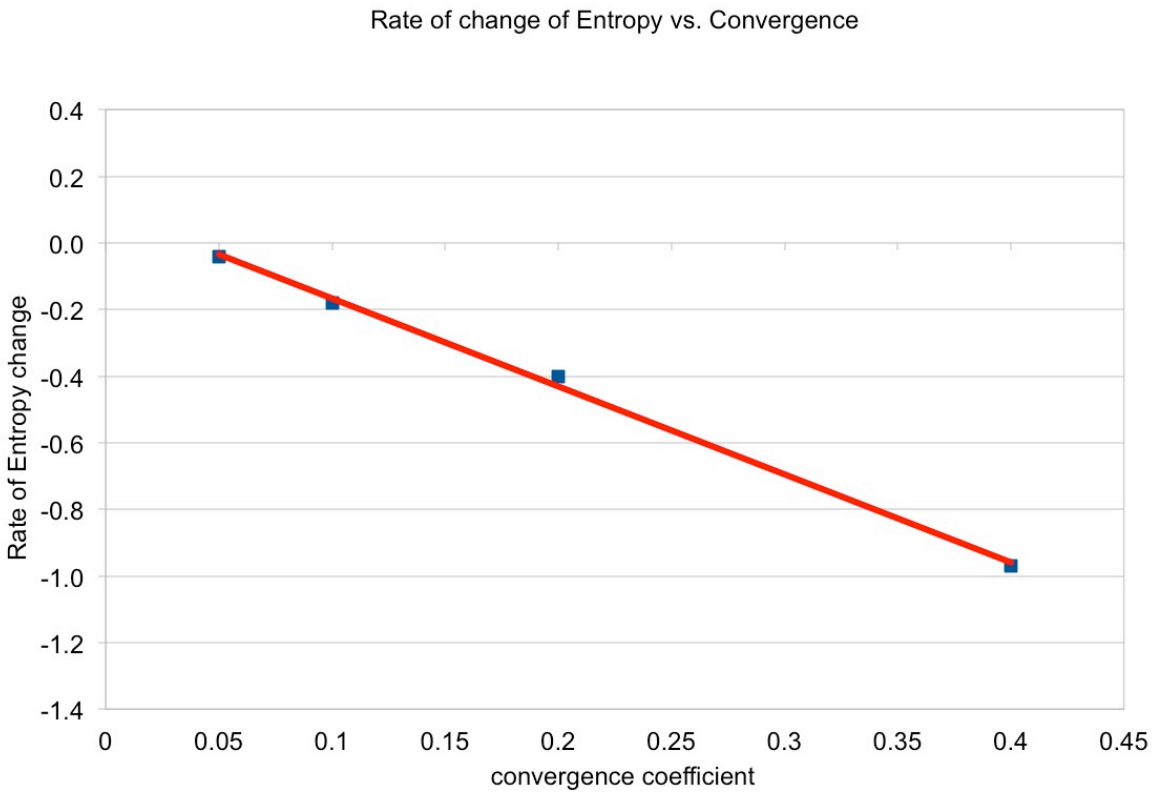

Figure 12. Beaching study of uniform random distribution

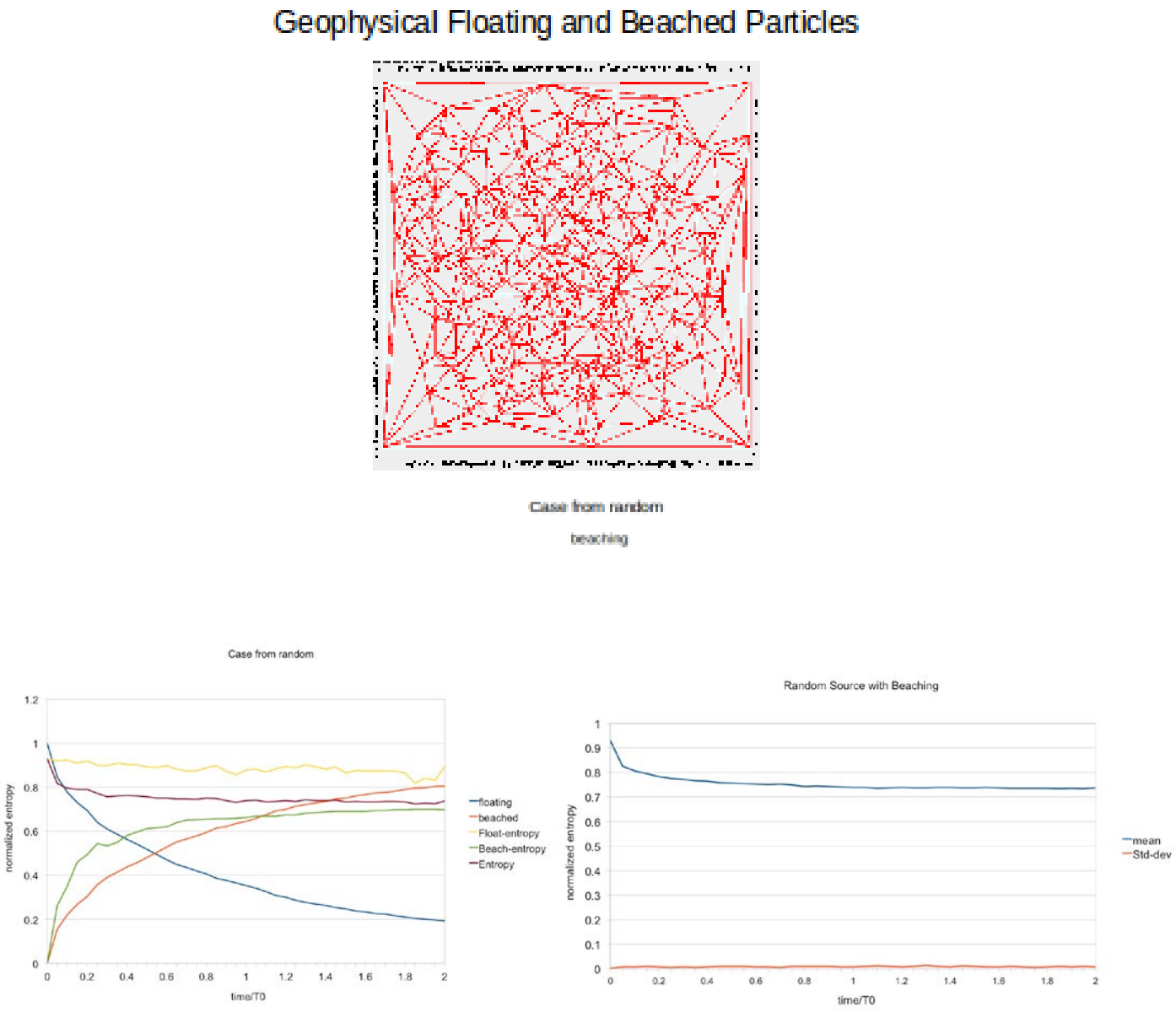

Figure 13. Beaching study of point source distribution

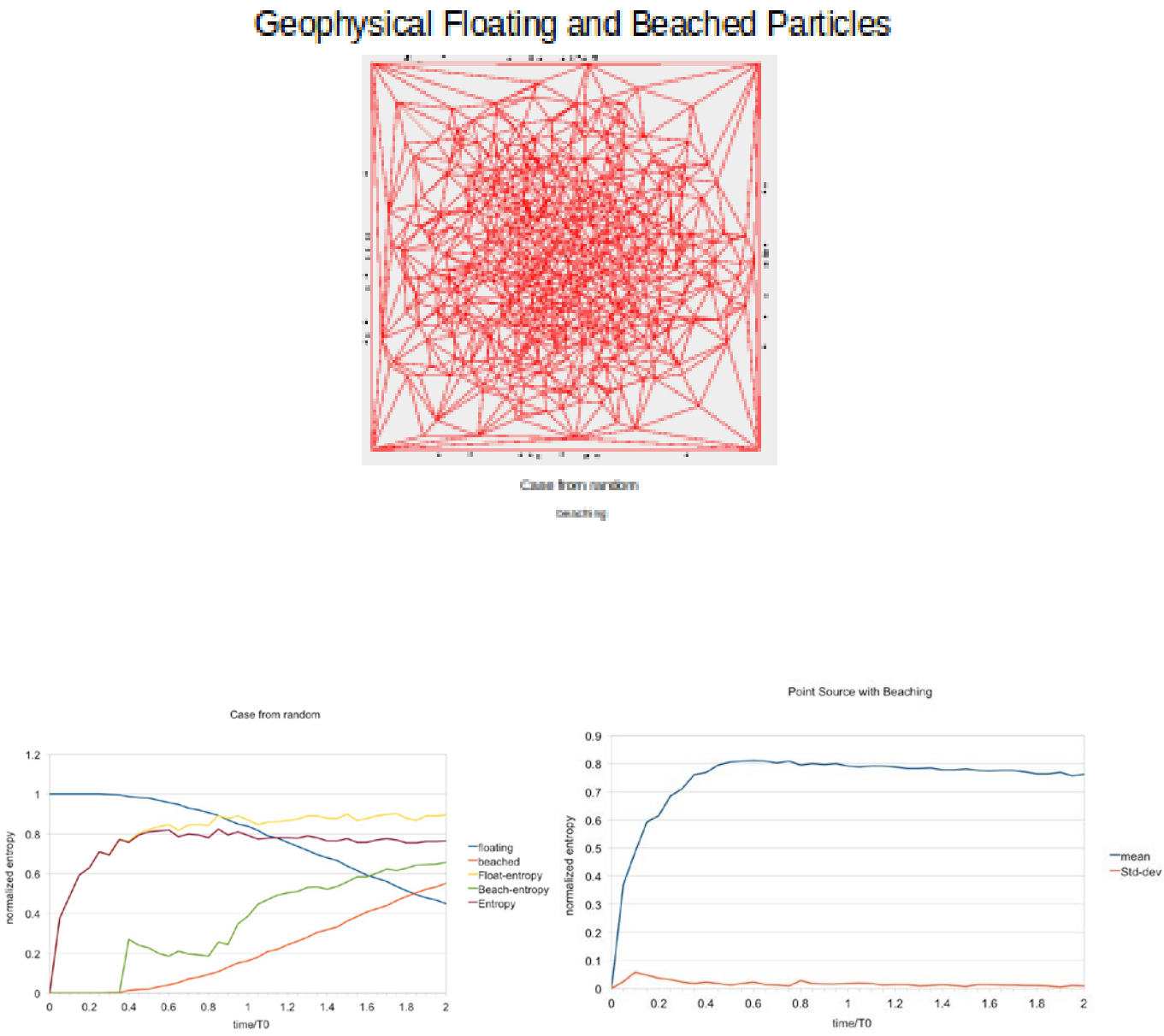

Figure 14. Beaching study of point source with advection

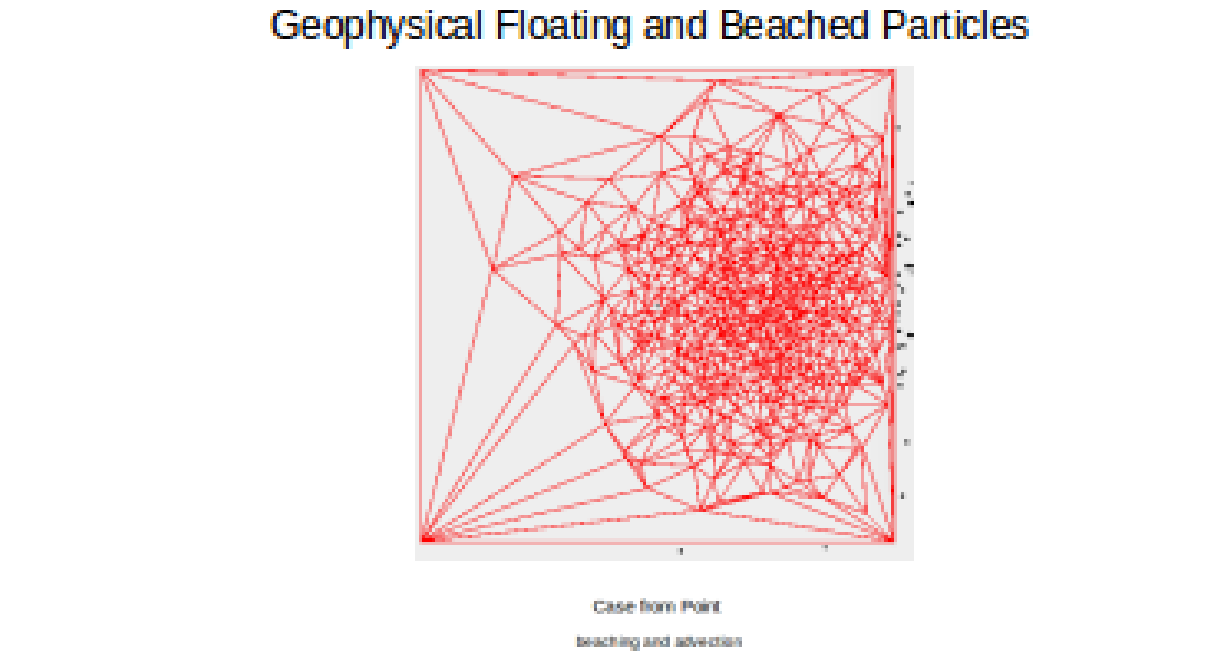

Figure 15. Model output at time T_0 for the cases where the convergence coefficient is first 0.1 (convergence) and then -0.1 (divergence).

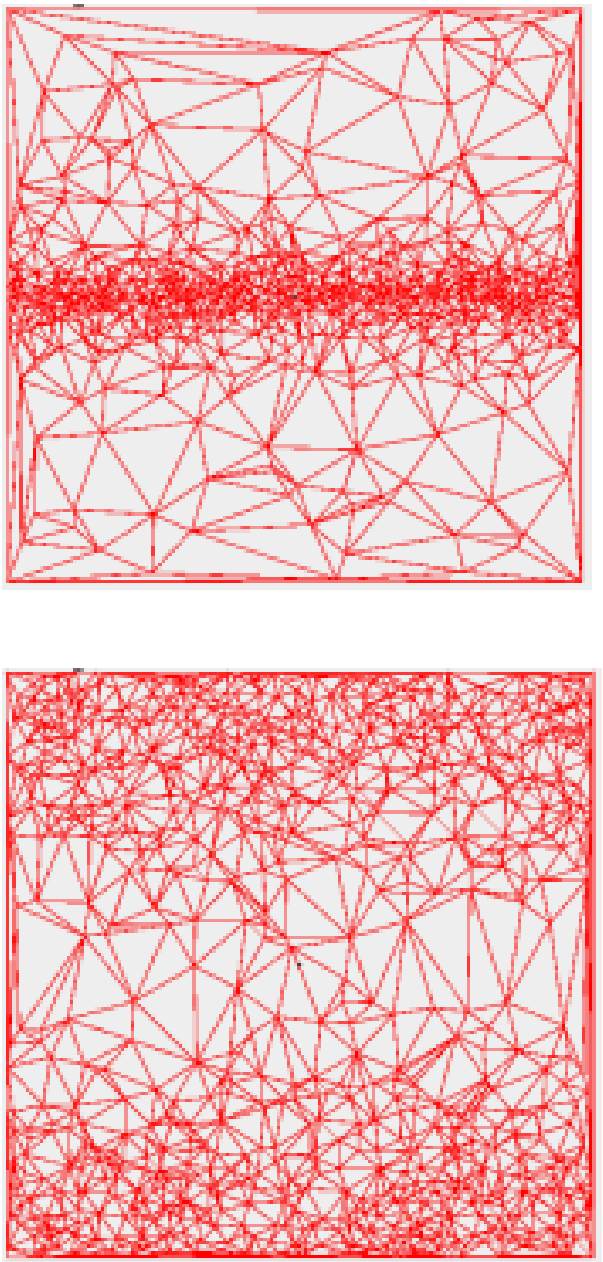

Figure 16. First-order components of differential motion around a point

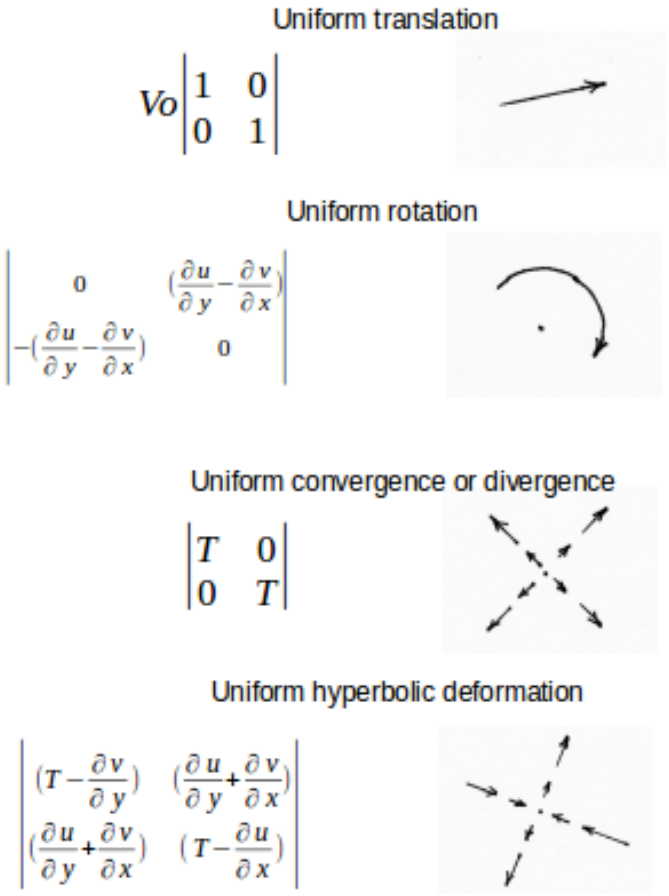

Figure – 17 Setup for localized change in entropy following an individual Lagrangian trajectory

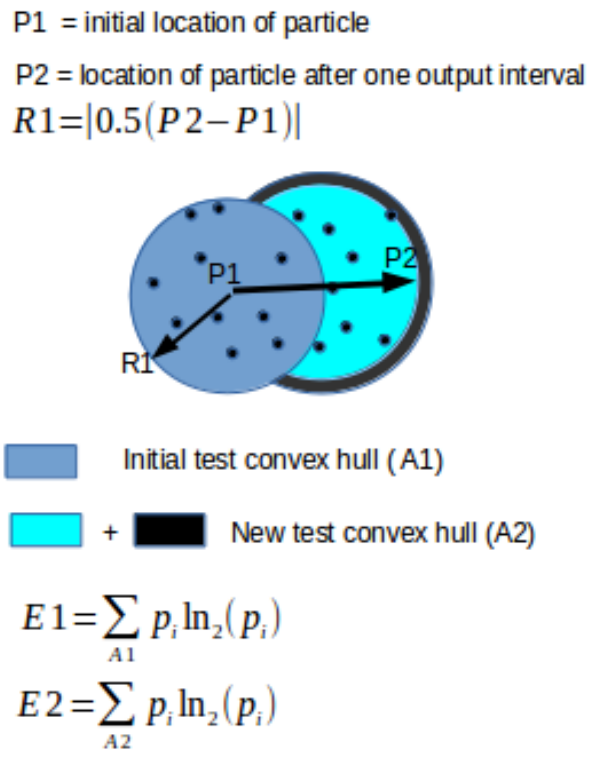

Figure 18. Three Trajectories used in Entropy Study

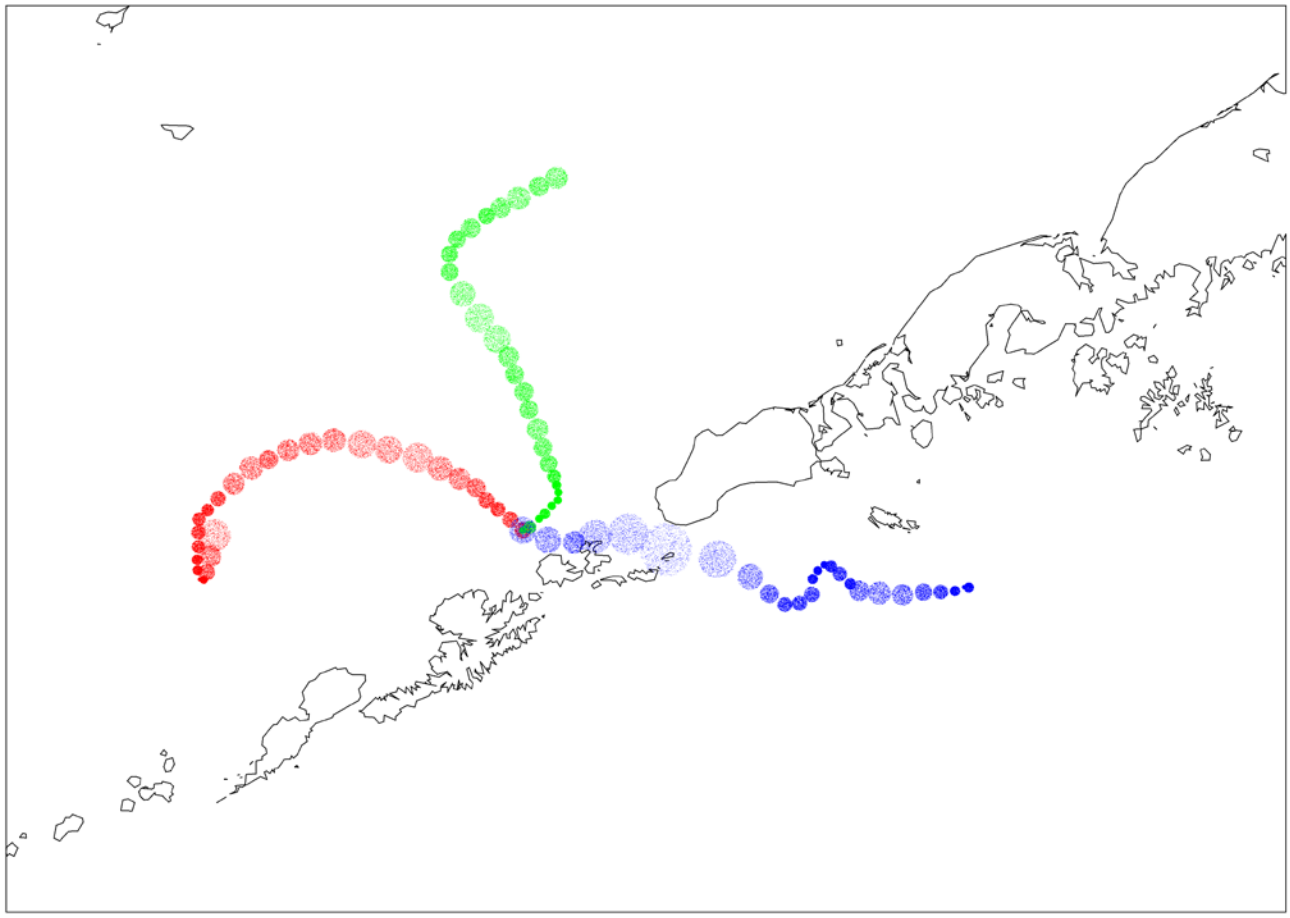

Track 1 (Red) – Bering Sea

Track 2 (Green) – Bering Shelf

Track 3 (Blue) – Unimak Pass

Figure 19. Track 1: change in entropy components for each time step

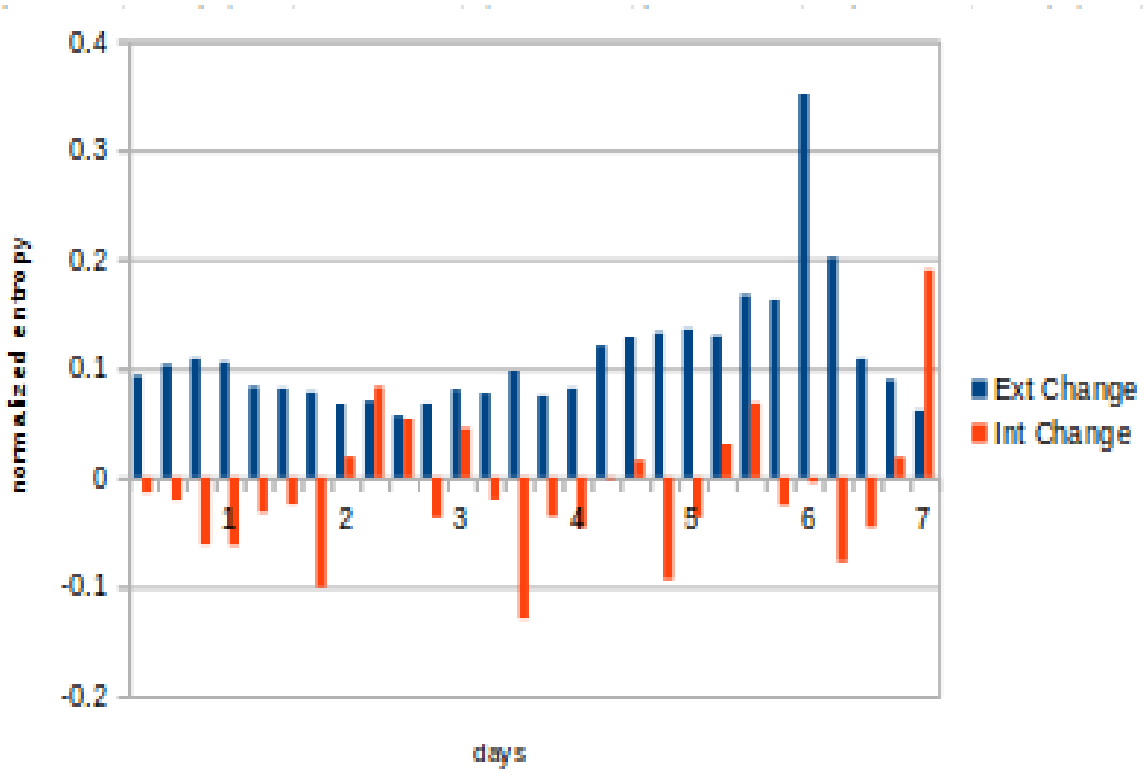

Figure 20. Track 1: Cumulative entropy change

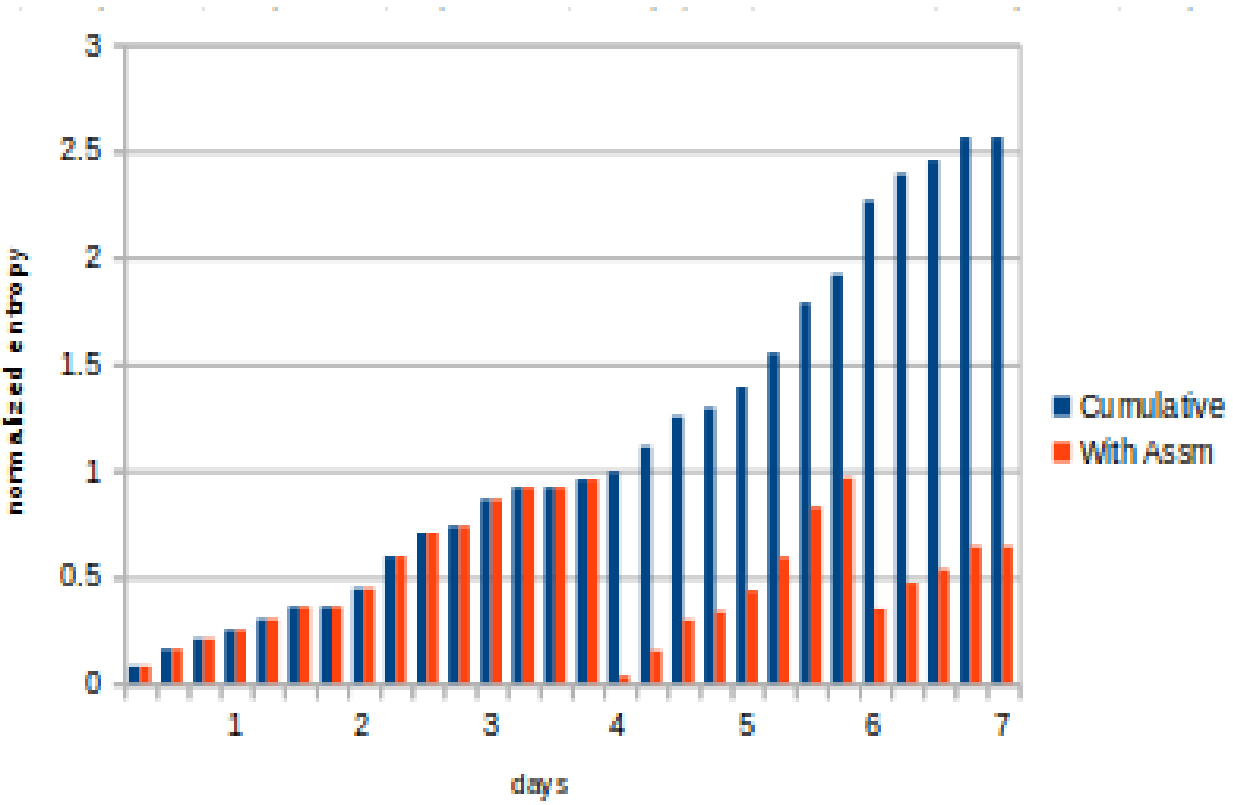

Figure 21. Track 2: change in entropy components for each time step

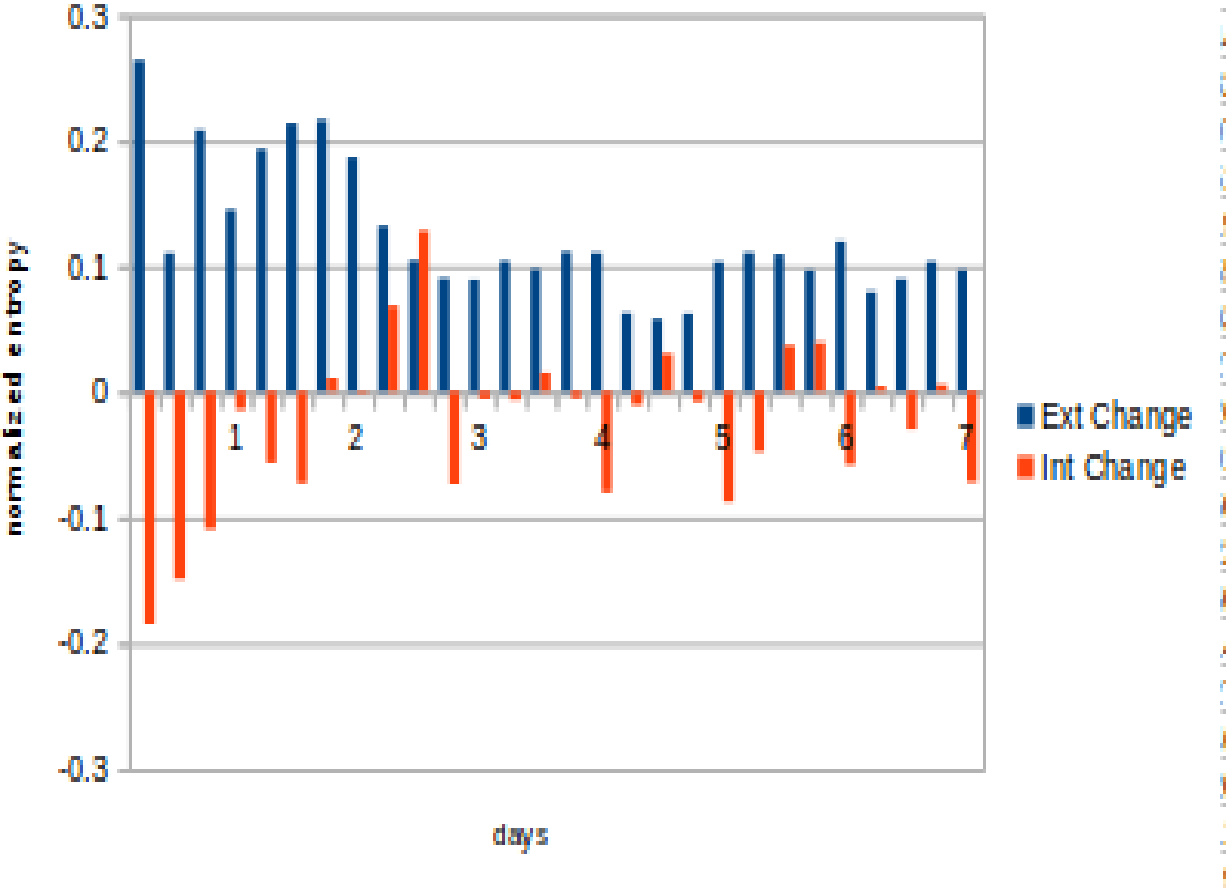

Figure 22. Track 2: change in entropy components for each time step with harmonics marked

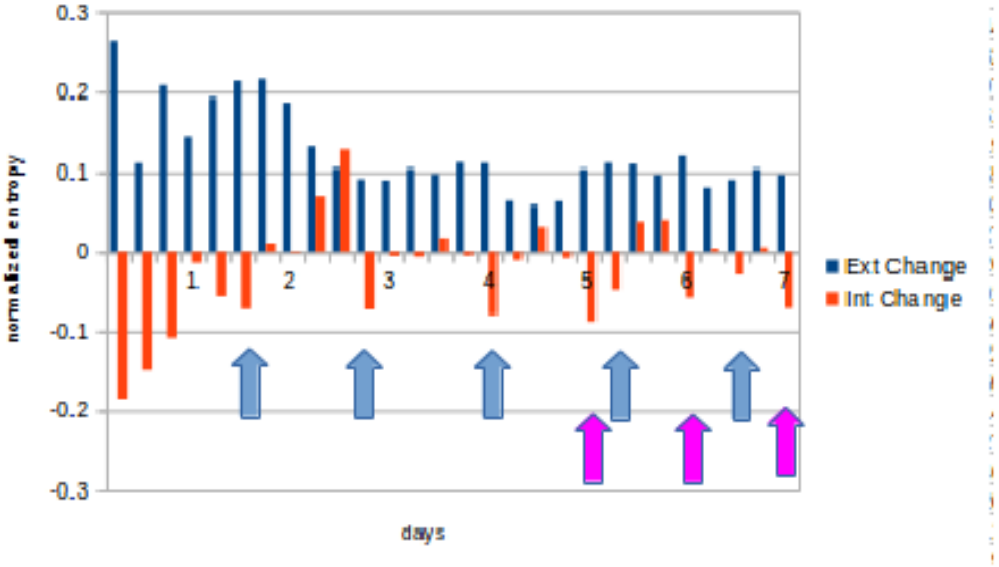

Figure 23. Track 2: Cumulative entropy change

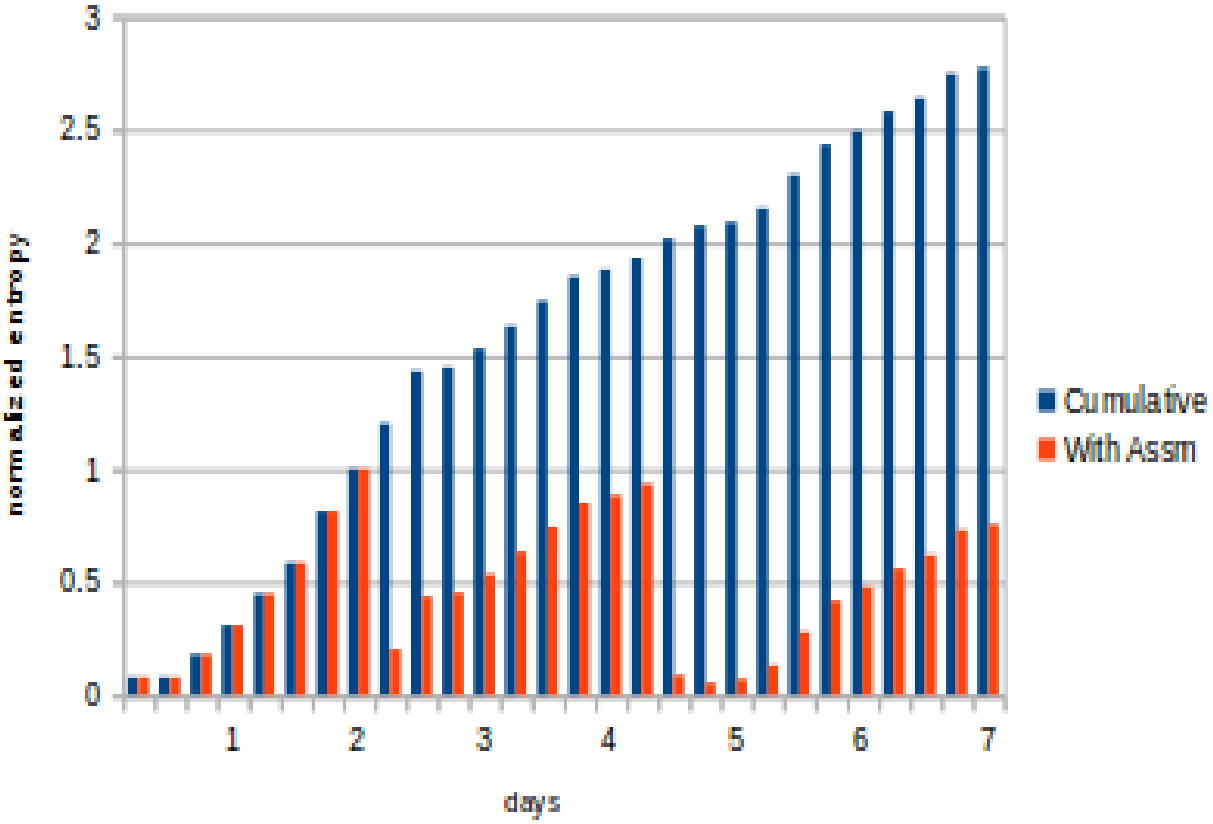

Figure 24. Track 3: change in entropy components for each time step

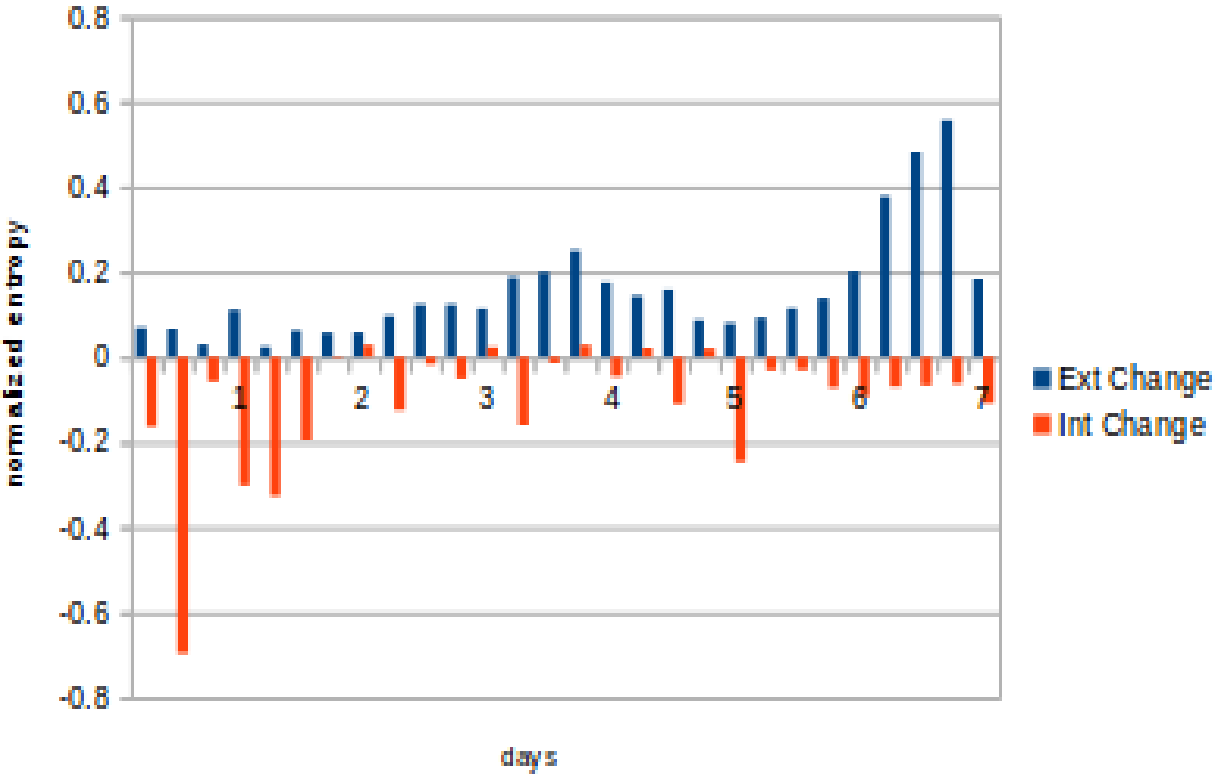

Figure 25. Track 3: Cumulative entropy change

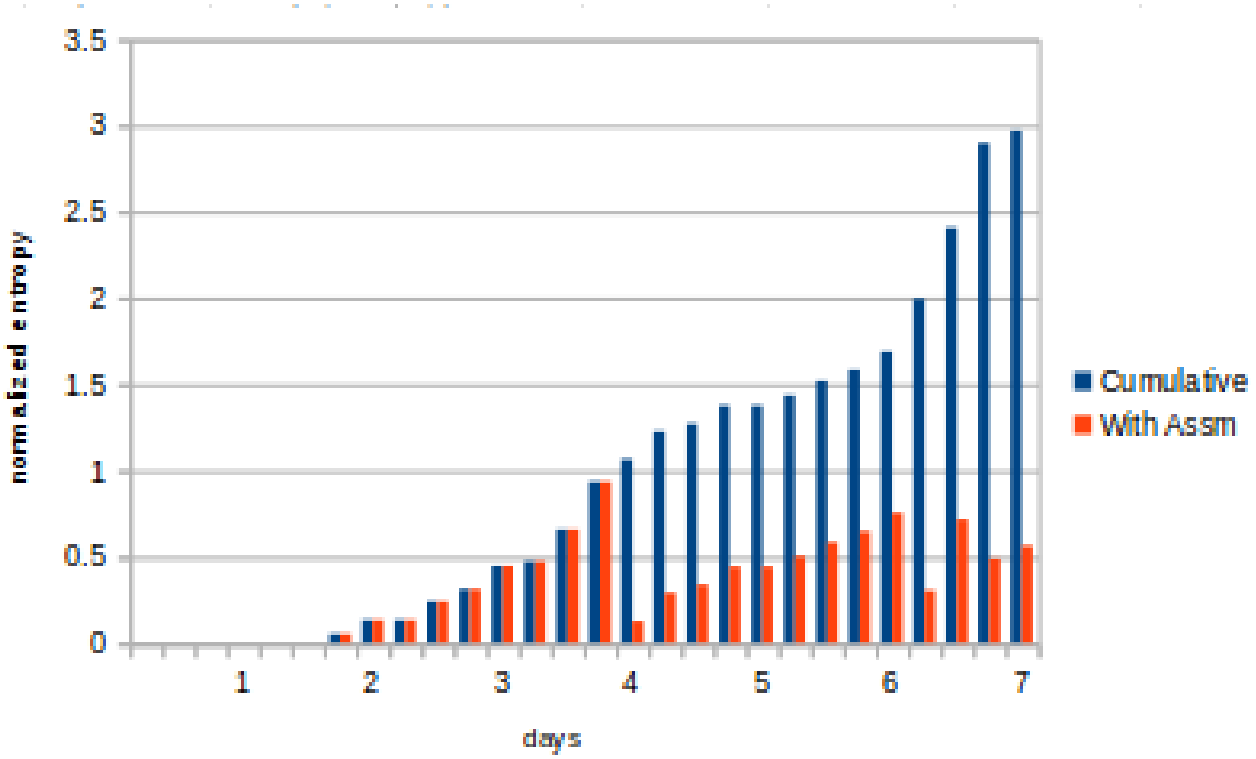

Appendix

Lagrangian particles as sets

Set definition

Consider a set (LE) which is made up of N elements. The N elements are partitioned into four subsets (S, F, B and O). Thus each subset contains some fraction of the N elements (n_i):

$$(n_i \in S) \vee (n_i \in F) \vee (n_i \in B) \vee (n_i \in O) \quad \text{(A1)}$$

and the cardinality of each of the subsets is between 0 and N subject to the restriction that:

$$N = S_n + F_n + B_n + O_n \quad \text{(A2)}$$

where the cardinality of each of the sets S_n, F_n, B_n, O_n are given by:

$$S_n = \sum_{n \in S} 1 \,;\, F_n = \sum_{n \in F} 1 \,;\, B_n = \sum_{n \in B} 1 \,;\, O_n = \sum_{n \in O} 1 \quad \text{(A3)}$$

Note that there is no restriction on the subsets' cardinality with the exception of the limits implied by equations A1 and A2. In particular, it is possible for one of the subsets to be empty, or to contain all of the elements.

The probability that an element is in any particular subset can be defined as:

$$\begin{aligned} S_p &= \frac{S_n}{N} \\ F_p &= \frac{F_n}{N} \\ B_p &= \frac{B_n}{N} \\ O_p &= \frac{O_n}{N} \end{aligned} \tag{A4}$$

And, from equations A1 and A4, the probability distribution over membership in subsets is:

$$\frac{\sum_i \left(S_p + F_p + B_p + O_p\right)}{N} = 1 \tag{A5}$$

A one to one mapping is defined for each subset such that each $n_i$is taken into a non-negative scalar:

$$D(n_i): \Rightarrow \rho_i \tag{A6}$$

The $D(n_i)$functions that are defined will, in general, be different for each of the subsets. (Where any confusion may occur a lower case subscript will be added to the definition in equation 6, for example $D_f(n_i)$ represents the mapping used for $n_i \in F$.)

We can also simplify the notation by the requirement that:

$$\begin{aligned} D_s(n_i) &= 0 for (n_i \notin S) \\ D_f(n_i) &= 0 for (n_i \notin F) \\ D_b(n_i) &= 0 for (n_i \notin B) \\ D_O(n_i) &= 0 for (n_i \notin O) \end{aligned} \tag{A7}$$

The D mapping is intended to represent a generalized Eulerian density function and from a dimensional analysis we expect density to be in the form of a "mass" divided by a "volume". The mass unit for this formulation is the mass (M_i) associated with the LEs in the Lagrangian trajectory formulation. It is unambiguous and common to all of the subsets. The "effective volume" ($effvol_i$) used in this function may be different in each of the subsets and is associated with a particular partition of the subset which assigns a neighborhood to each of the LEs $M_i$values.

Using equations A6 and A7 we can define a local (set specific) Eulerian density within each subset as:

$$\rho_i = \frac{M_i}{effvol_i} \tag{A8}$$

From equation A8 a local probability is defined as:

$$prob(n_i) = \frac{\rho_i effvol_i}{\sum_i \rho_i \, effvol_i} \tag{A9}$$

Which is plainly the local density times its associated effective volume (neighborhood) normalized by its sum over the entire domain. From equation A7 and A8 the summation over the entire domain will be bounded by the summation over the particular subset containing the LE. In addition the summation probabilities over any subset will be unity.

$$\sum_i prob\,(n_i) = 1 \tag{A10}$$

Recognizing that D mapping may have a different definition in each of the subsets the overall probability of n_i which could occur in any of the four subsets will be the conditional probability:

$$prob(n) = \left\{\frac{S_n}{N}\right\}\left\{\frac{\rho_i effvol_i}{\sum_i \rho_i\, effvol_i}\right\} + \left\{\frac{F_n}{N}\right\}\left\{\frac{\rho_i effvol_i}{\sum_i \rho_i\, effvol_i}\right\} + \left\{\frac{B_n}{N}\right\}\left\{\frac{\rho_i effvol_i}{\sum_i \rho_i\, effvol_i}\right\} + \left\{\frac{O_n}{N}\right\}\left\{\frac{\rho_i effvol_i}{\sum_i \rho_i\, effvol_i}\right\} \tag{A11}$$

A pictorial representation of the set is shown as:

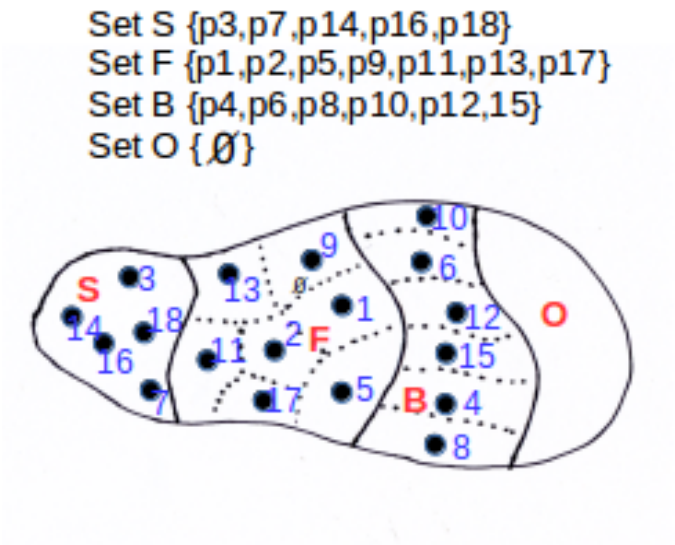

Examples

This set and it's definitions of probability may seem a bit contrived, however, there are a number of examples where it provides a useful description.

Example 1: Colored and numbered beads

In this initial example we may notice that the probabilities are described in two levels. If we were to have N colored beads, representing four groups, (S, F, B, O) placed into a jar, the probability of randomly drawing one from color group S would be $S_p = S_n/N$. If, in addition, we were to number each of the beads 1 though N and define $D(n_i) = 1$ for all the subsets, the probability of a randomly selected bead being "n" will depend on the conditional probability of first being in a particular subset and then depending on the density distribution within that subset.

$$prob(n) = \left\{\frac{S_n}{N}\right\}\left\{\frac{1}{\sum_s 1}\right\} + \left\{\frac{F_n}{N}\right\}\left\{\frac{1}{\sum_f 1}\right\} + \left\{\frac{B_n}{N}\right\}\left\{\frac{1}{\sum_b 1}\right\} + \left\{\frac{O_n}{N}\right\}\left\{\frac{1}{\sum_o 1}\right\} \tag{A12}$$

From equation A7 we see that three of the four terms in the left hand side of equation A12 will be zero and the remaining term reduces to:

$$prob(n) = \frac{1}{N} \tag{A13}$$

Which is just what we would expect given that the numbering system gave each element an equal D value and was independent of the subset.

Example 2: Multiple alphabet cryptogram

A slightly more complex example of this set is its representation of a cryptogram that uses four different alphabets (say Greek, Latin, Hebrew and Cyrillic). Their relative frequency within the cryptogram is represented by the subsets. Within each of the alphabets, the frequency of letters appear in a known ratio. For example, in English there are many more e's and t's than w's and q's. These ratios form the basis for defining the D mappings. With this set up, a cryptanalysis of the expected probability distribution of letters could be checked against observation and a Bayesian attack used as the basis for solving the cryptogram. In this case the individual letter probabilities will be:

$$prob(n) = \left\{\frac{S_n}{N}\right\}\left\{\frac{\rho_i freqS_i}{\sum_i \rho_i\, freqS_i}\right\} + \left\{\frac{F_n}{N}\right\}\left\{\frac{\rho_i freqF_i}{\sum_i \rho_i\, freqF_i}\right\} + \left\{\frac{B_n}{N}\right\}\left\{\frac{\rho_i freqB_i}{\sum_i \rho_i\, freqB_i}\right\} + \left\{\frac{O_n}{N}\right\}\left\{\frac{\rho_i freqO_i}{\sum_i \rho_i\, freqO_i}\right\} \quad \text{(A14)}$$

Any single letter probability results in a value that depends on the fraction of times a particular alphabet is used and the probable occurrence of letters within the alphabet. It should also be clear that:

$$\sum_i prob\,(n_i) = 1 \quad \text{(A15)}$$

Lagrangian Trajectory Model

We now shift our focus to a Lagrangian trajectory model and, to be specific, we consider a particle tracking formulation of some segment of a realistic geophysical marine environment. As a particular model we specify GNOME (General NOAA Operational Modeling Environment) which is used to track oil spills and is in the public domain. Any number of common particle tracking models could be represented by this set model.

The GNOME model allows the user to specify the pollutant as a number (N) of individual particles referred to as LEs (Lagrangian Elements). These particles are assumed to represent an unspecified, but particular mass of pollutant. Initially all of the LEs are contained (in a ship – set S) and may be moving through the domain. A spill scenario is developed where some fraction of the LEs are released from the ship (become floating – set F) into the marine environment. The release may be instantaneous or variable over time and space within the domain. Various transport processes, such as winds and currents will move the floating LEs and at some point they may become stranded along one of the shorelines specified in the model domain (on a beach - set B). Stranding can be reversed in the sense that LEs may rewash from a

beach and rejoin the floating population of LEs (back into set F from set B). It is also possible that environmental transport processes carry LEs to an open boundary of the model domain and they then are and no longer part of the scenario under study (off the map - set O). As the GNOME spill model runs, it provides a time stepping record of: 1) LEs not released (S), 2) LEs floating (F), 3) LEs beached (B), and 4) LEs that are off the map (O). Thus, as the model runs through its scenario it provides time dependent data populating the LE sets defined above. Each of the subsets is well defined and although set members can transition from one subset to another the overall constraints of the LE set and its contained subsets are enforced by the basic continuity requirements of GNOME (or any proper surface transport model).

To complete the formulation of the LE set, the mapping (D) shown in equation A6 and A7 must be defined for each of the S, F, B, and O subsets. From the probability function (equation A9) it is also evident there is a link between the individual definition of D and the sum of the values over all of the D_n subsets. This means that the generalized density value is actually normalized for each of the subsets, and there is really only one degree of freedom left, and it is associated with "effective volume" specificity within that set. The obvious meaningful choices for volume specificity are: one (All of the LE's in the subset are thought of as resident in a single container.); and, $n \in set$. (Each of the LEs in the subset are thought of as resident in their own partition of the subset.) Using these two possibilities the D functions can be defined.

Subset S – ship

$$D_s(n_i) = \rho_{sn} = M_i/n_i \tag{A16}$$

The S_n LEs that are in the ship each make up a fraction of the "volume", the total of which adds to a single volume. From a locational point of view the S (ship) subset is thought of as a single undifferentiated location. We might notice that most tank ships are divided into a number of separate tanks, but oil spill trajectory models like GNOME do no distinguish the individual tanks.

Subset F – floating

The target space for the floating LEs is the entire water region represented by the scenario under study. The water surface area of the model is partitioned into individual sub areas ($poly_i$) associated with one of the LEs in the F subset. The ratio of these sub area (sq. km.) segments will, in some sense, be related to the Eulerian neighborhood of the LE it is associated with.

$$D_f(n_i) = \rho_{fi} = M_i/poly_i \tag{A17}$$

The F LEs may be scattered in any fashion whatsoever over the water surface of the model domain, and surrounding it is an associated area that represents its neighborhood. The density function (A17) then represents a normalized local Eulerian density. From a dimensional point of view D_f is mass/area. This is appropriate since the floating surface on which LEs move is 2-dimensional.

Subset B – beached

The target space for the beached LEs is the entire shoreline, or all the non-open boundaries represented by the scenario under study. For the B subset, the shoreline will be partitioned into individual length segments (seg_i) each of which incorporates one of the B LEs. The collection of each of these segments will make up the specificity associated with the subset B. That is, there will be exactly B_n segment seg_i lengths defined on B.

$$D_b(n_i) = \rho_{bi} = M_i/seg_i \tag{A18}$$

From a dimensional point of view, D_b is mass/length. This then explains what was meant by the term “generalized area” mentioned above. The appropriate metric for shoreline is length, not area, so that is what is seen in equation A18. Although this may seem a bit strange there is nothing in the definition of the LE set that requires that the D mappings be the same for each subset and, as can be seen the different subsets, may be

over dimensionally unrelated domains.

Subset O – off map

The final subset O is simple. It represents a repository for all of the LEs that are transported outside of the region represented for the scenario under study. This will be pollutant mass that we no longer have any information on. We know the mass of the material we are no longer tracking, but it only has a single regional attribute "gone". In this sense, the O subset is somewhat like the S subset, and has a single undifferentiated location. This leads to the following:

$$D_o(n_i) = \rho_{on} = M_i/n_i \tag{A19}$$

Once LEs are off of the map their location is not specified, other than gone.